AGU PUBLICATIONS

Water Resources Research

RESEARCH ARTICLE

10.1002/2016WR018716

Transferring measured discharge time series: Large-scale comparison of Top-kriging to geomorphology-based inverse modeling

A. de Lavenne[1,2], J. O. Skøien[3], C. Cudennec[4,5], F. Curie[1], and F. Moatar[1]

[1]Université Francois Rabelais - Tours, EA 6293, Géo-Hydrosystèmes Continentaux, Faculté des Sciences et Techniques, Tours, France, [2]Now at Irstea, Hydrosystems and Bioprocesses Research Unit, Antony, France, [3]European Commission, Joint Research Centre, Institute for Environment and Sustainability, Climate Risk Management Unit, Ispra, Italy, [4]AGROCAMPUS OUEST, UMR1069, Sol Agro et hydrosystème Spatialisation, Rennes, France, [5]INRA, UMR1069, Sol Agro et hydrosystème Spatialisation, Rennes, France

Key Points:

- The geomorphological inversion approach and Top-kriging are equally efficient for continuous streamflow simulation
- Small upstream catchments have higher uncertainties than larger catchments for both methods
- A rescaled Ghosh distance provides the best weighting of donor catchments for geomorphological inversion

Supporting Information:

- Supporting Information S1

Correspondence to:
A. de Lavenne,
alban.de-lavenne@irstea.fr

Citation:
de Lavenne, A., J. O. Skøien, C. Cudennec, F. Curie, and F. Moatar (2016), Transferring measured discharge time series: Large-scale comparison of Top-kriging to geomorphology-based inverse modeling, *Water Resour. Res.*, *52*, doi:10.1002/2016WR018716.

Received 5 MAR 2016
Accepted 15 JUN 2016
Accepted article online 17 JUN 2016

Abstract Few methods directly transfer streamflow measurements for continuous prediction of ungauged catchments. Top-kriging has been used mainly to predict the statistical properties of runoff but has been shown to outperform traditional regionalization approaches of rainfall-runoff models. We applied the Top-kriging approach across the Loire River basin and compared predictions to a geomorphology-based approach. Whereas Top-kriging uses spatial correlation, the other approach has the advantage of being more physically based by using a well-known geomorphology-based hydrological model (WFIUH) and its inversion. Both approaches require an equal degree of calibration and provide similar performances. We also demonstrate that the Ghosh distance, which considers the nested nature of catchments, can be used efficiently to calculate weights and to identify the suitability of gauged catchments for use as donor catchments. This result is particularly relevant for catchments with Strahler orders above five, i.e., where donor catchments are more strongly nested.

1. Introduction

The previous IAHS decade on "Predictions in Ungauged Basins" (PUB) resulted in a large amount of literature on the issue of ungauged catchments [*Sivapalan et al.*, 2003; *Hrachowitz et al.*, 2013; *Blöschl et al.*, 2013]. Regionalization techniques are a deeply studied subset of methods.

Different definitions of "regionalization" exist; in runoff hydrology, the term generally refers to methods for interpolating hydrological information to ungauged catchments [*He et al.*, 2011]. Most often this is achieved by assessing hydrological similarities or developing statistical relations between the desired variables, parameters and easily observable catchment characteristics.

Among the regionalization approaches for predicting continuous streamflow, few methods transfer direct observations of the variable of interest. Most are based on rainfall-runoff models that are applied in both gauged and ungauged locations, and regionalization techniques are then used to interpolate the calibrated model parameters [see for instance *Vandewiele et al.*, 1991; *Merz and Blöschl*, 2004; *Oudin et al.*, 2008, 2010]. One limitation of the approach is that, in addition to the uncertainty in the estimated parameters, issues inherent in the model itself are also transferred (simplifying hypotheses, issues related to parameters' identification, rainfall uncertainty, etc.).

An alternative approach which avoids these problems, and which can be applied when the causal rainfall-runoff relation is not needed, is to regionalize streamflow properties directly. The greatest limitation in most cases is the uncertainty in magnitude and spatial distribution of rainfall for both the gauged and ungauged catchments. Runoff observations also naturally integrate human influence, such as dams or water withdrawals for irrigation, which is challenging to model consistently.

Several observation-based approaches found in the literature rely on geostatistical techniques to spatially interpolate variables measured in the stream network [*Skøien et al.*, 2006; *Isaak et al.*, 2014; *Müller and Thompson*, 2015; *Farmer*, 2016]. Topological kriging (or Top-kriging) of a variety of variables was recently compared to several other methods. *Archfield et al*. [2013] demonstrated that Top-kriging substantially outperformed a regression approach (with observable catchment descriptors) and canonical kriging (physiographical space-based interpolation) in estimating flood quantiles of 61 catchments in the southeastern United States. *Laaha et al*. [2014] also compared Top-kriging with the traditional regression approach for 300 Austrian catchments to estimate low flow quantiles. They showed that Top-kriging generally performed better, or at locations without upstream observations, as well as the regression approach. Recently, *Müller and Thompson* [2015] also evaluated their own kriging strategy, called TopREML, in a comparison with Top-kriging. They demonstrated similar performances for mean streamflow and runoff frequency but better predictions of model uncertainties.

Kriging has sometimes also been used to interpolate runoff time series. *Farmer* [2016] used ordinary kriging at a daily time step, whereas *Skøien and Blöschl* [2007] extended their topological kriging technique for this purpose at an hourly time step. *Viglione et al*. [2013] demonstrated that this spatiotemporal Top-kriging also outperforms regionalized rainfall-runoff models for the daily streamflow prediction of 213 Austrian catchments.

Patil and Stieglitz [2012] also directly transferred daily streamflow time series in the U.S. and weighted donor catchments using inverse-distance weighting (IDW) between stream gauges. They used the prediction performance to identify regions where nearby catchments tend to have similar streamflow patterns and demonstrated that spatial proximity between donor and receiver catchments alone cannot fully explain the prediction performance at a given location.

An alternative method to transfer hydrograph measures was developed by *Andréassian et al*. [2012]. They developed simple equations (from one to three parameters) that facilitate the transfer of daily and hourly streamflow time series. They averaged predictions from seven donor catchments and demonstrated that this approach, which they called “nature’s own hydrological model,” was as efficient as a calibrated rainfall-runoff model.

Originally formulated by *Cudennec* [2000] and then applied to different contexts [*Boudhraâ*, 2007; *Boudhraâ et al*., 2006, 2009; *de Lavenne et al*., 2015], a geomorphology-based inverse/direct modeling approach transfers an observed hydrograph of a gauged catchment to ungauged catchments, either nested, neighboring or similar. This work is based on estimating net rainfall from runoff discharge measurements, which facilitates direct transfer.

Following the idea that transferring direct measurements is an attractive alternative for several practical PUB issues, the aim of this study was twofold: (1) to explore the geomorphology-based approach for a large number of catchments, beyond the methodological validation for a small number of gauged catchments that had already been performed; (2) to compare Top-kriging and the geomorphology-based approaches for predicting continuous streamflow. We facilitated this comparison by using a similar calibration approach and distance functions for all catchments. The analyses were performed on a comprehensive dataset for the Loire River basin, the largest French basin (117,500 km^2), which provides a range of cascading and parallel gauged subbasins with high geographic heterogeneity.

2. Methods

Both approaches were analyzed with the statistical environment R [*R Core Team*, 2015]. Top-kriging was previously implemented in the rtop package [*Skøien et al*., 2014] and was extended for this study to also perform topological kriging of time series.

Before we present the two methods in more detail, a general overview (Figure 1) emphasizes that both approaches require similar input variables and parameters but use them in different ways. Parameterization of both approaches is initially related to water transfer in time and along flow paths, which is partly responsible for different hydrograph shapes among catchments. The geomorphology-based approach deconstructs and reconstructs each discharge time series signal using the unit hydrograph (UH) principle and by using an intermediate variable, which is net rainfall (details in section 2.3). Any UH can be estimated from analyzing hydraulic length over the entire catchment (x_c) and a mean channel velocity (u_c). Conversely, Top-kriging does not require evaluating intermediate hydrological variables or describing catchment geomorphology. Top-kriging runs directly with discharge time series that are synchronized by considering the lag time caused by water flowing between outlets along x_c and at a similar estimated velocity u_c. The core of the method is a geostatistical model that describes the spatial variability of discharge to optimize its interpolation (details in section 2.2).

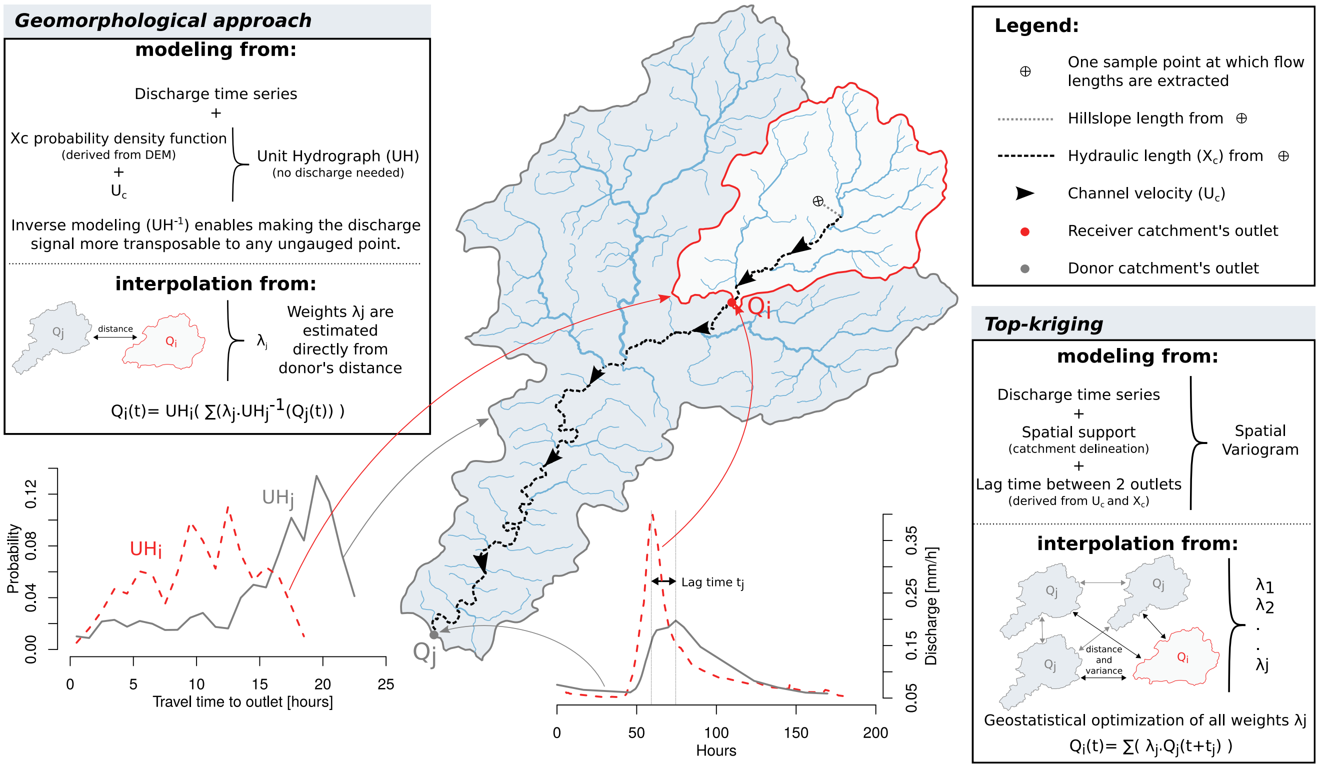

Figure 1. Conceptual comparison and input variables used by the two approaches for transferring discharge time series.

2.1. Velocity Estimation and Rising Times

Both approaches require estimating only one parameter: streamflow velocity u_c. We regionalized this parameter and used it identically in both approaches to facilitate their comparison. Based on the work of *de Lavenne* [2013], we applied an algorithm to detect and extract rising times T_{Ri} of catchment i from its observed runoff. The algorithm analyzes runoff time series to find noticeable rises.

This analysis is based on two main criteria: (1) slope of the rise: relative change in runoff per time step must exceed 0.75% h^{-1} at the beginning of the rising limb and 0.1% h^{-1} during the rising limb; (2) surface runoff volume and intensity: the area under the runoff curve during the rising limb, and greater than the first run-off value of the event, is used to approximate the amount of flowing water. Its volume must be greater than 0.005 mm and its intensity more than 0.004 mm h^{-1}. Because the hydrograph can have a complex rise (i.e., with small fluctuations), a rising limb is identified when discharge increases during a period of six time steps. The rising limb is considered to end when discharge decreases for more than 8 h.

Streamflow velocity is then estimated from the mean hydraulic length and the rising times T_{Ri}.

$$u_c^i = \frac{\overline{x_c}}{T_{Ri}} \tag{1}$$

The multiple estimates of streamflow velocity enabled a regional relation between rising times and stream-flow velocity to be determined (Figure 2):

$$u_c = a \cdot \overline{x_c}^{\,b} \tag{2}$$

where $a = 4.38 \times 10^{-4}$ and $b = 0.69$.

2.2. Spatiotemporal Kriging Method

2.2.1. Top-Kriging

Top-kriging can be seen as a combination of two processes inside a geostatistical framework that controls the streamflow. The first is continuous in space and corresponds to runoff generation, which mainly depends on rainfall, evapotranspiration and soil characteristics. This variable is conceptualized by a point

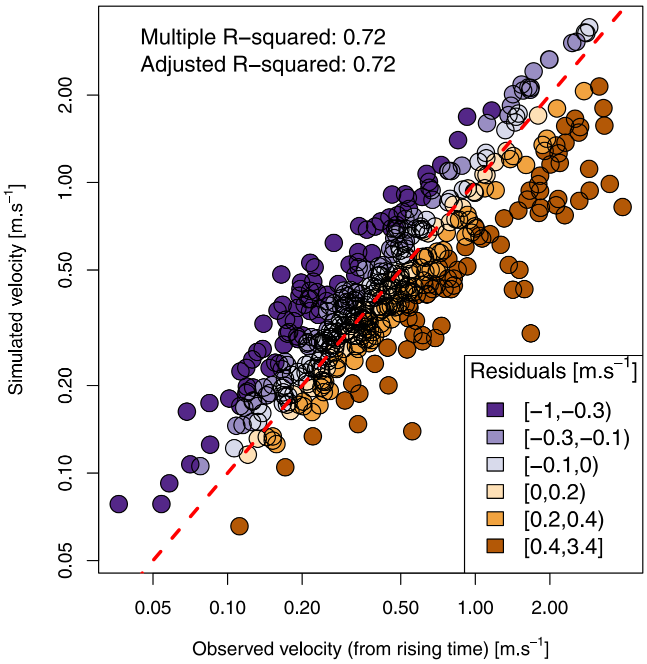

Figure 2. Comparison of velocity estimated from regression and velocity estimated from rising time.

process that is assumed to exist over the entire catchment. This variability in a geostatistical framework can be described by Euclidean distances, and its spatial statistical characteristics are represented by a variogram [*Skøien et al.*, 2006]. Generated runoff ($z(A_1), z(A_2),\ldots, z(A_n)$) cannot be observed continuously in space but is observed as a spatial aggregate at stream gauges where

$$z(A_i)=\frac{1}{|A_i|}\int_{A_i} z(x)dx \tag{3}$$

and A_i is the spatial support of $z(A_i)$. For streamflow variables, A_i is the upstream area of a catchment that drains into a river location x_i, and $|A_i|$ is its surface area.

The second variable is the flow routing in the stream network. It results from the accumulation and aggregation of runoff along the network, such as those in nested catchments. This variable is defined by one point in the stream network, which is the outlet of the catchment. Contrary to the first variable, it cannot be represented by Euclidean distances but needs a method that reflects the tree structure of the stream network.

Top-kriging aims to integrate these two aspects, which define the hydrological response of one catchment, to interpolate streamflow-related information between catchments. *Skøien and Blöschl* [2007] interpolated runoff time series by conceptualizing the aggregate at the outlet as the convolution of the runoff generated within the catchment during the time needed by the generated runoff to reach the outlet. In this study we assume that, after calibration, an integrated spatial variogram is numerically similar to an integrated space-time variogram, similar to that developed by [*Skøien et al.*, 2006]. We applied Top-kriging to runoff time series by assuming that runoff is only spatially correlated with time series [*Kyriakidis and Journel*, 1999]. For each time step t_ω, specific runoff $\hat{q}(x_i, t_\omega)$ of an ungauged target catchment defined by location x_i is estimated from observed specific runoff $q(x_j, t_\alpha)$ at the same time step $t_\alpha = t_\omega$ of neighboring gauged catchments located at x_j as

$$\hat{q}(x_i, t_\omega)=\sum_{j=1}^{n}\lambda_j q(x_j, t_\alpha) \tag{4}$$

From the hypothesis of stationarity and the randomness of runoff generation processes, optimal weights λ_j can be found by solving the kriging system:

$$\begin{aligned} &\sum_{k=1}^{n}\lambda_k\gamma_{jk}-\lambda_j\sigma_j^2+\mu=\gamma_{ij} \qquad j=1,\ldots,n \\ &\sum_{j=1}^{n}\lambda_j=1 \end{aligned} \tag{5}$$

where the gamma values γ_{ij} and γ_{jk} are the expected semivariances between the ungauged catchment i and the neighbors j used for estimation, and between two neighbors j and k, respectively. The variable μ is the Lagrange parameter, and σ_i^2 represents the measurement error or uncertainty in measurement i.

Because measurements are related to a nonzero support A, the semivariance γ_{ij} between two measurements with catchment areas A_i and A_j must be obtained from regularization [*Cressie*, 1993]. Also, because

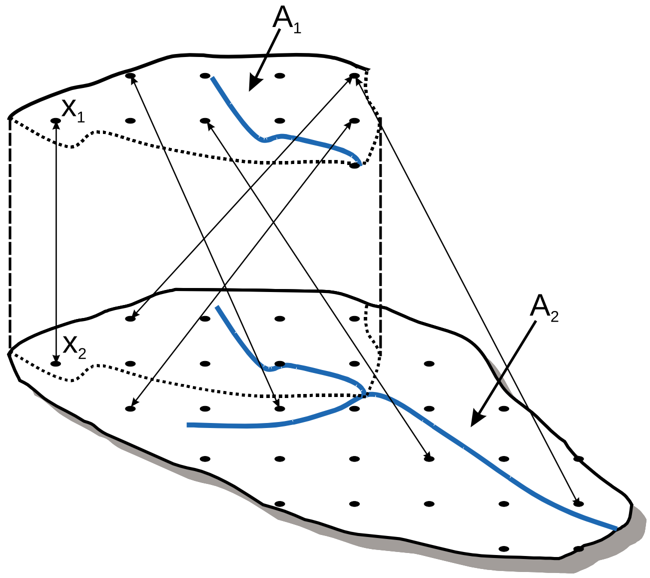

Figure 3. Discretization of two catchment areas A_1 and A_2 using points x_1 and x_2 to evaluate distances [from *Skøien et al.*, 2006].

the size of the drained area increases from upstream to downstream, the transfer of information from one outlet to another implies a change of support. For this reason, the variogram model must be regularized for each combination of catchment areas. This accounts for the different scales and nested nature of the catchments. Assuming the existence of a point semivariogram γ_p, the expected semivariance γ_{ij} between two observations of catchment areas A_i and A_j is

$$\begin{aligned}\gamma_{ij} &= 0.5 \cdot Var(z(A_i) - z(A_j)) \\ &= \frac{1}{A_i A_j}\int_{A_i}\int_{A_i} \gamma_p(|x_1 - x_2|)dx_1dx_2 - 0.5 \cdot \left[\frac{1}{A_i^2}\int_{A_i}\int_{A_j}\gamma_p(|x_1-x_2|)dx_1dx_2 + \frac{1}{A_j^2}\int_{A_j}\int_{A_j}\gamma_p(|x_1-x_2|)dx_1dx_2\right]\end{aligned} \tag{6}$$

where x_1 and x_2 are position vectors within each catchment used for integration. The first part of equation (6) finds the mean of the point variogram between the two catchments. The second part generates a smoothing effect by subtracting the mean of the point variogram within the two catchments. This formulation considers the nested nature of two catchments: their semivariance will decrease as the overlap of their support increases. To facilitate the calculation, the integrals in equation (6) are replaced by sums, and catchment areas are discretized by a regular grid (Figure 3).

To simplify the calculation, *Gottschalk* [1993] and *Gottschalk et al.* [2011] suggested applying the covariance model to the mean distance between areas, d^*_{ij}, instead of calculating the covariance for each distance and then calculating the mean.

$$d^*_{ij} = \frac{1}{|A_i||A_j|}\int_{A_i}\int_{A_j}(|x_i - x_j|)dx_i dx_j \tag{7}$$

We henceforth refer to this distance as the *Ghosh* [1951] distance. The regularized semivariance between two areas then simply becomes

$$\gamma^*_{ij} = \gamma_p(d^*_{ij}) - 0.5 \cdot (\gamma_p(d^*_{ii}) + \gamma_p(d^*_{jj})) \tag{8}$$

where d^*_{ii} represents the mean distances within A_i.

2.2.2. Top-Kriging of Time Series

Skøien and Blöschl [2007] extended the Top-kriging approach to address runoff time series. Based on the analysis of *Skøien and Blöschl* [2006], which described catchment behavior as a space-time filter, *Skøien and Blöschl* [2007] developed spatiotemporal Top-kriging to consider space and time correlation of runoff time series along the stream network.

This approach considers routing within a catchment but not between catchments. Consequently, *Skøien and Blöschl* [2007] developed a simple routing model that considers the time shift caused by water flowing from an upstream to a downstream catchment.

Skøien and Blöschl [2007] demonstrated that this routing, combined with spatial kriging, yielded predictions better than those of spatiotemporal kriging. On this basis, we implemented spatial kriging, as previously described, but supplemented it with a simple routing routine. It should be noted that this assumption is an appropriate choice for a regular time series, but that full spatiotemporal kriging is necessary when time series are irregular, if the degree of intermittency in the time series is high, or if the intention of the interpolation is to increase the temporal resolution of the time series.

The routing routine consists of estimating the time shift that may be observed between catchments, which is due to advection and hydrological dispersion [*Rinaldo et al.*, 1991]. Thus, we estimate $\hat{q}(x_i, t_\omega)$ from the neighboring observations $q(x_j, t_\alpha^*)$ at time steps $t_\alpha^* = t_\alpha + t'_\alpha$ instead of t_α in equation (4), where t'_α reflects the time shift or difference in response time of the two catchments.

There are several ways to estimate this time shift. One option is to calculate the time shift $t'_{ij\alpha}$ between catchments i and j, as the difference between regionalized rising times for the studied region (see section 2.1 above for more details). The time shift is then estimated from the difference between their estimated rising times T_{Li} and T_{Lj}:

$$t'_{ij\alpha} = T_{Lj} - T_{Li} \tag{9}$$

where T_{Li} and T_{Lj} are respectively the rising times of catchments i and j. It is important to note that $t'_{ij\alpha}$ can be negative.

To estimate the effect of the routing, we also performed an alternative variant of Top-kriging in which the time shift was set to zero.

$$t'_{ij\alpha} = 0 \tag{10}$$

Both rising time estimates are found from equation (11).

$$T_{Li} = \frac{\overline{x_c}}{u_c} \tag{11}$$

where $\overline{x_c}$ is the mean hydraulic length, and u_c is the streamflow velocity estimated by equation (2).

We consider T_{Li} and T_{Lj} an approximation of catchment response time, an approximation of the time needed by rainfall to trigger the main streamflow response of catchments i and j. If we assume spatially homogeneous rainfall over the catchments, $t'_{ij\alpha}$ is thus equivalent to the time separating their peak flows. This approach may be more realistic than focusing only on the time needed by water to flow from one outlet to another within the river network (which then requires distinguishing nested/nonnested catchments). A downstream catchment does not receive water only from upstream river flow but also from its own hillslopes and other tributaries. Considering only streamflow travel time may underestimate the time shift separating two catchments. Conversely, T_{Li} and T_{Lj} are influenced by travel time through hillslopes; so, their difference consequently also considers hillslope travel time (the effect depends on the catchment size; see for instance *D'Odorico and Rigon* [2003]), whereas the opposite is the case for higher Strahler orders.

2.2.3. Choice of Variogram Model

We chose the nonstationary version of the exponential variogram model because *Skøien et al*. [2006] demonstrated that it works well for interpolating hydrological data and because it has few parameters.

2.3. Transferring Hydrograph by the Width Function Inversion Method

This method was originally formulated by *Cudennec* [2000]. It was applied in a semiarid context in Tunisia [*Boudhraâ*, 2007; *Boudhraâ et al*., 2006, 2009] and more recently in oceanic temperate France [*de Lavenne*, 2013; *de Lavenne and Cudennec*, 2015; *de Lavenne et al*., 2015].

2.3.1. A Geomorphology-Based Model

As discussed by *Robinson et al*. [1995] and similar to Top-kriging, this approach distinguishes runoff generation over hillslopes (production function) from flow routing in the stream network (transfer function). The approach focuses only on the transfer function, which is built from a morphometric description of the flow path within

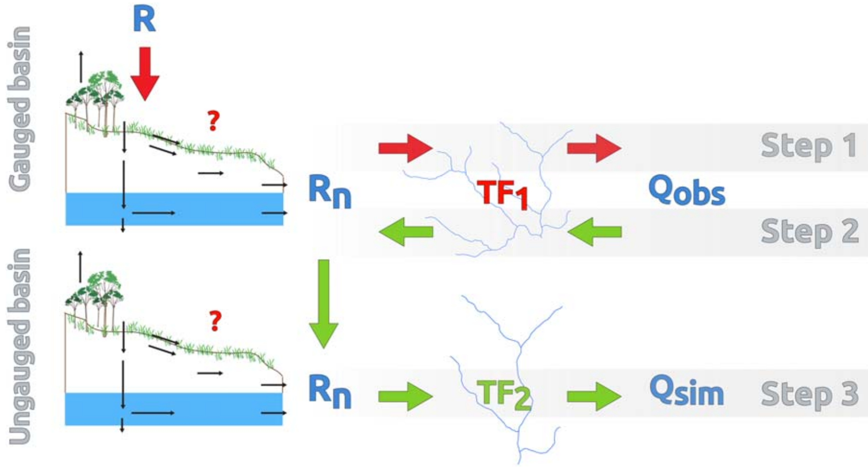

Figure 4. Principle of direct transfer of a hydrograph [from *de Lavenne and Cudennec*, 2015].

the river network [*Cudennec et al.*, 2004; *Cudennec and Fouad*, 2006; *Cudennec*, 2007; *Aouissi et al.*, 2013]. The hydraulic length x_c, defined as the distances to the outlet from any point within the river network, is estimated from a digital elevation model (DEM) of the catchment and is described as a probability density function ($pdf(x_c)$) of distances. Assuming a linear transfer function throughout the river network [*Naden*, 1992; *Beven and Wood*, 1993; *Blöschl and Sivapalan*, 1995; *Robinson et al.*, 1995; *Yang et al.*, 2002; *Giannoni et al.*, 2003b, 2003a; *Rodriguez et al.*, 2005], an estimate of a mean channel flow velocity (u_c) provides the *pdf* of water travel time t through the river network. This *pdf* is a transfer function and can be referred to as the Unit Hydrograph ($UH(t)$). This geomorphology-based UH is also usually called the WFIUH (Width Function Instantaneous Unit Hydrograph) in the literature. To facilitate the comparison with Top-kriging, we used the same approach to estimate channel flow velocity and the regression described by equation (2).

Assessing $UH(t)$ allows estimation of discharge at the outlet Q (m^3 s^{-1}) (Step 1, Figure 4) using the following convolution:

$$Q(t)=S\cdot\int_0^t R_n(t-\tau)\cdot UH(\tau)\cdot d\tau \tag{12}$$

where t (s) is time, S (m^2) is the catchment's surface area, R_n (m) is net rainfall, and τ is a temporal integration variable.

2.3.2. Deconvolution and Transfer of the Hydrograph

In the original application, the hydrograph of the closest gauged catchment is transferred onto an ungauged catchment using net rainfall as an intermediate variable. Net rainfall R_n is defined as the depth of runoff provided by a catchment's hillslope into its river network; thus, it is a theoretical concept that exists independent of rainfall and as long as there is water in the stream. It is estimated from the gauged catchment and transferred onto an ungauged catchment. The approach assumes that for a pair of nested or neighboring catchments, the net rainfall of the gauged catchment (donor catchment) can represent the net rainfall of the ungauged one (receiver catchment). This assumption comes from the idea that net rainfall is more independent of catchment size than the hydrograph itself, and that the shape of the hydrograph is influenced by the size and geometry of the catchment. In other words, assessing the net rainfall time series solves the scaling issue underlying the transfer of hydrographs.

The hydrograph measured at the outlet of one gauged catchment is used to estimate its net rainfall through a deconvolution of the signal. This is achieved by inverting the gauged catchment's geomorphology-based transfer function (Step 2, Figure 4). In this manner, the net rainfall time series is estimated from the discharge time series. Step 3 of the approach (Figure 4) is to transfer this net rainfall onto an ungauged catchment and to perform a convolution with the ungauged catchment's transfer function. This is achieved using equation (12), and the resulting time series is the predicted hydrograph. It is important to note that because the approach is based only on the catchment's transfer function, it does not need to include a production function. This would involve a more complex modeling approach to describe the highly nonlinear hillslope behaviors.

Table 1. Parameter Values Used to Inverse the Transfer Function of Each Basin

Ad	Ap	Bd	Bp	Dd	Tp
0.01	0.9	0.01	0.001	1	20

2.3.3. Net Rainfall Estimation

The objective of the deconvolution is to assess the net rainfall time series R_n that best reconstitutes the measured discharge time series Q_m, according to the model *UH*. It is an inverse problem because one knows the model and its output; one is looking for its inputs. This inversion is solved by minimizing the following equation [*Tarantola and Valette*, 1982; *Menke*, 1989]:

$$(Q-Q_m)^T \cdot (C_Q^m)^{-1} \cdot (Q-Q_m)+(R_n-R_n^{ap})^T \cdot (C_{Rn}^{ap})^{-1} \cdot (R_n-R_n^{ap}) \tag{13}$$

where Q is the output of the model, R_n^{ap} is initial a priori information about R_n, C_{Rn}^{ap} and C_Q^m are covariance matrices for vectors R_n^{ap} and Q_m, respectively. The estimate of R_n^{ap} comes from the specific discharge Q_m, to which a delay equal to the catchment's rising time is applied.

According to the inverse-problems theory [*Tarantola and Valette*, 1982; *Menke*, 1989] and following previous implementation of this approach [*Boudhraâ*, 2007; *Boudhraâ et al.*, 2006, 2009], a maximum likelihood solution allows net rainfall to be estimated:

$$R_n=R_n^{ap}+C_{Rn}^{ap} \cdot UH^T \cdot (UH \cdot C_{Rn}^{ap} \cdot UH^T+C_Q^m)^{-1} \cdot (Q_m-UH \cdot R_n^{ap}) \tag{14}$$

Six parameters must be estimated to calibrate the covariance matrices: *Ad*, *Ap*, *Bd*, *Bp*, *Dd*, and *Tp*. These parameters quantify the errors related to Q_m and R_n^{ap}, which are assumed to be zero-centered Gaussian distributed (see *Cudennec* [2000] and *Boudhraâ* [2007] for more details about these parameters). Their values were fixed manually (Table 1) based on the results of *de Lavenne* [2013].

2.3.4. Transposition Strategy

It has been demonstrated that this approach can be further extended to combine hydrographs of several gauged catchments [*de Lavenne*, 2013; *de Lavenne and Cudennec*, 2015]. This is done to perform either ensemble prediction (see Figure 15 later) or a mean simulation from several gauged catchments.

$$R_n^i=\sum_{j=1}^{n} \lambda_j \cdot R_n^j \tag{15}$$

where R_n^i is the estimated net rainfall of ungauged catchment i, R_n^j is the simulated net rainfall of gauged catchment j from inversion, λ_j is the weight of gauged catchment j, and n is the number of gauged catchments considered in the transfer.

To help compare this approach to Top-kriging, we fixed $n=5$ for both methods and estimated λ_j for each gauged catchment by exploring four different weighting strategies: (1) a simple mathematical mean of the donor's net rainfall (which is equivalent to equal weights), (2) an inverse-distance weighting (IDW) based on centroid distances, (3) an inverse rescaled Ghosh distance (equation (17), described below), and (4) the optimized weights obtained from applying Top-kriging.

We defined a rescaled Ghosh distance Γ_{ij}^* similar to the Top-kriging approach, as presented in equation (8), using a linear variogram $\gamma(h)=h$:

$$\Gamma_{ij}^*=d_{ij}^*-0.5 \cdot (d_{ii}^*+d_{jj}^*) \tag{16}$$

Table 2. Quantiles of Goodness of Fit of Simulations According to Four Criteria[a]

	NS_Q			r			NS_{lnQ}			VE		
	25%	50%	75%	25%	50%	75%	25%	50%	75%	25%	50%	75%
Inversion (centroid IDW)	0.58	0.78	0.88	0.86	0.92	0.95	0.64	0.81	0.89	0.59	0.72	0.80
Inversion (Ghosh IDW)	0.65	0.82	0.91	0.88	0.93	0.96	0.69	0.85	0.92	0.64	0.75	0.82
Inversion (no weights)	0.55	0.75	0.86	0.86	0.91	0.94	0.62	0.78	0.87	0.58	0.70	0.76
Inversion (Top-kriging weights)	0.64	0.80	0.90	0.87	0.92	0.96	0.69	0.83	0.91	0.63	0.73	0.81
Top-kriging (no routing)	0.66	0.81	0.91	0.88	0.92	0.96	0.70	0.83	0.91	0.63	0.74	0.82
Top-kriging (with routing)	0.68	0.82	0.91	0.88	0.93	0.96	0.70	0.84	0.91	0.63	0.75	0.82

[a] NS_Q: Nash-Suttcliff efficiency, NS_{lnQ}: Nash-Suttcliff efficiency with logarithm transformation, r: Pearson correlation, VE: volumetric efficiency, and IDW: inverse-distance weighting.

This aims to improve the calculation of distance between hydrological variables with two-dimensional supports (catchment areas) [*Ghosh*, 1951; *Gottschalk*, 1993; *Gottschalk et al*., 2011]. As an approximation of the Top-kriging approach, we applied an inverse function to this rescaled Ghosh distance to estimate the weights of the donor catchments:

$$\lambda_{ij} = \frac{1}{\Gamma^*_{ij}} \cdot \frac{1}{\sum_{k=1}^{n} (1/\Gamma^*_{kj})}$$
$$\sum_{k=1}^{n} \lambda_{kj} = 1 \qquad (17)$$

where λ_{ij} is the weight of gauged catchment i used to estimate the net rainfall of ungauged catchment j, and n is the number of gauged catchments considered in the transfer. The second equation in the set of equations (17) allows λ_{ij} to vary between 0 and 1, and to sum up to 1. In addition, as a hybrid model, we extracted the weights of donor catchments estimated by Top-kriging and applied them when transferring net rainfall.

As in our application of Top-kriging, we constrained the geographic extent in which gauged catchments were selected. Centroids of gauged catchments had to be located within a 50 km radius of the centroid of the ungauged catchment. The closest catchments were chosen when more than $n=5$ catchments were located within this radius. We used the centroids' geographic distance for weighting approaches (1) and (2), and the rescaled Ghosh distance for weighting approaches (3) and (4). When no catchment centroids existed within this radius, the catchment centroid with the shortest rescaled Ghosh distance was used.

3. Application

3.1. Cross Validation

To examine the relative performances of models more quantitatively, we performed leave-one-out cross-validation. After withholding the streamflow time series of a particular gauge, we predicted the time series for that location, and then compared the prediction to the streamflow observations. This procedure was repeated for all gauges and emulated prediction at sites without streamflow observations.

3.2. Efficiency Assessment

We evaluated the goodness of fit of predictions using four criteria: (1) NS_Q, the Nash-Sutcliffe criterion [*Nash and Sutcliffe*, 1970], which emphasizes errors on high flows; (2) NS_{lnQ}, the Nash-Sutcliffe criterion performed on log-transformed discharges, which emphasizes errors on low flows; (3) r Pearson correlation, which is used to evaluate timing correlation; and (4) VE, the volumetric efficiency developed by *Criss and Winston* [2008] as an alternative to the Nash-Sutcliffe criterion, which emphasizes the bias on water volume. The optimal value of all criteria is equal to 1. The Nash-Sutcliffe criterion has no lower bound, whereas r and VE have lower bounds equal to -1 and 0, respectively.

These criteria were calculated for all available runoff data, whose duration varied by catchment, as described in section 3.4.

3.3. Morphometric Description

To extract catchment boundaries and to analyze the flow path length required to build the UH (section 2.3), we used GRASS 7.0 supplemented by the toolkit of *Jasiewicz and Metz* [2011]. The hydraulic length x_c^i of catchment i is estimated over its entire area from a DEM at 25 m resolution. The D8 algorithm was used to model drainage, and a predefined river network provided by the *Sandre/BD CARTHAGE* database was burned into the DEM using an algorithm based on the inverse distance to the network [*Nagel et al*., 2011].

3.4. Studied Catchments and Data

Both modeling approaches were applied to the ensemble of all Loire catchments. We chose the most downstream outlet, near the city of Mont-Jean-sur-Loire, which drains a surface of about 110,000 km^2 and is

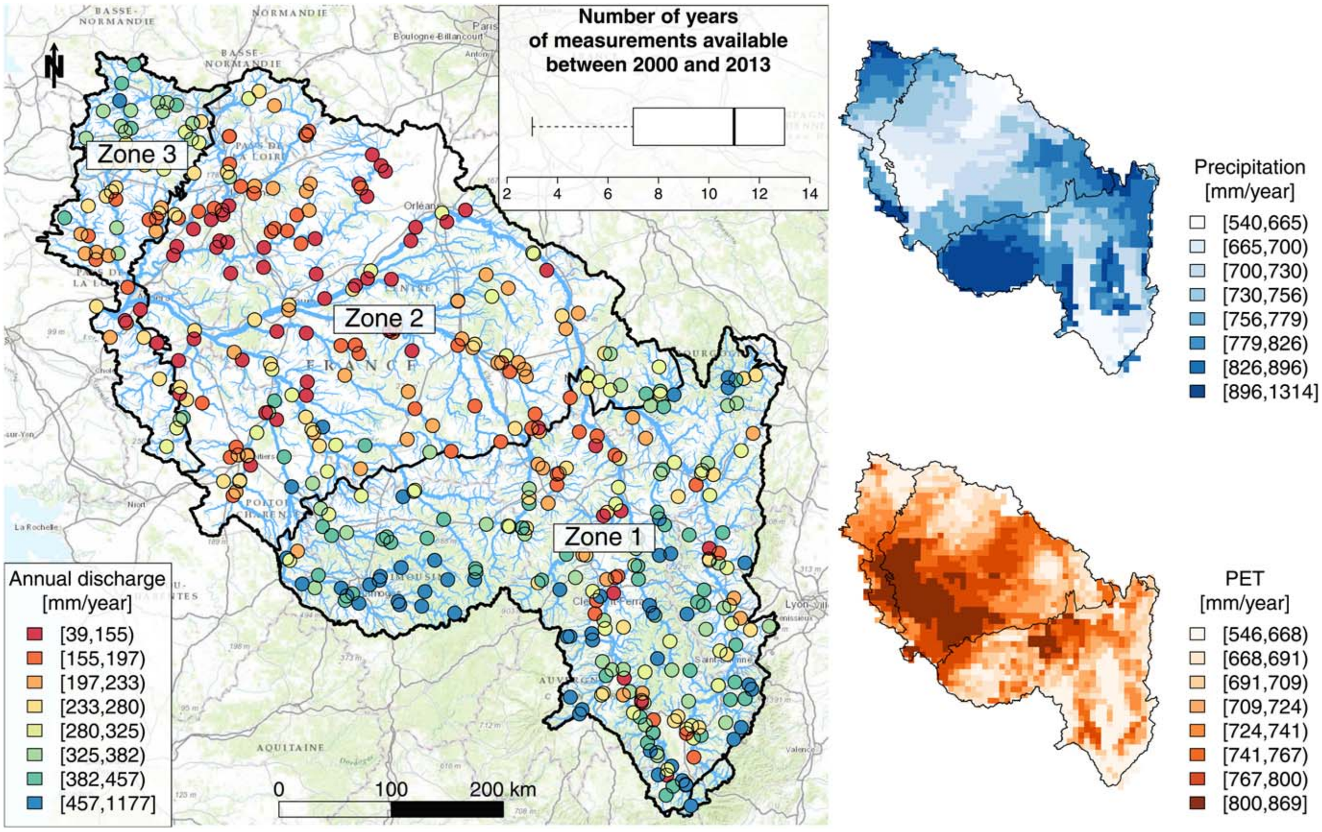

Figure 5. Specific annual discharge of the Loire catchments (Banque hydro database) with annual precipitation and potential evapotranspiration (PET) from the SAFRAN database (Météo-France). Statistics come from the 2000–2012 time period.

not influenced by tides. The catchment has high climatic, geological and hydrological variability. The catchment also has a varied climate (oceanic and continental) and lithology.

Three main regions are usually distinguished according to their lithology (Figure 5). The first is a mountainous region with a mean elevation of 800 m. It is defined mostly by granite and basalt bedrock. Catchments at higher altitudes have a nival influence. Its specific discharges are generally higher than those of the other regions because of more rainfall (from 500 to $>$1250 mm/yr) and its lithology, which favors surface runoff. The second region is located on sedimentary rocks and has contrasting hydrological behavior, especially due to a large aquifer connected to the river system. Its annual rainfall is lower, averaging 690 mm/yr. The third region is composed of granite and basalt and receives an average of 750 mm of rainfall per year.

For 87% of 184 stations analyzed by *Sauquet et al*. [2008] in the Loire catchment, pluvial river flow regimes dominated. In the mountainous region, only 12% of stations have a transition (pluvio-nival) regime, in which seasonal variation in streamflow is affected as much by precipitation timing as by air temperature and topographic influences (on snowpack formation and snowmelt timing). Typically, high flows are observed in spring. One percent of stations in the southern part of the Loire catchment are representative of Mediterranean river flow regimes, with low flow in summer and high flow in November. The snowmelt-fed regime is not observed in the Loire catchment. Some stations are influenced by one or more reservoirs which are located in the mountainous region: 10% are influenced throughout the year and 8% only during low flow. The two largest dams (totaling 350 Mm^3) are Naussac (low flow moderation) and Villerest (low flow moderation and flood control). Other, smaller dams (totaling 200 Mm^3) are used to generate hydropower.

Discharge measurements were extracted from the French Hydro Database (www.hydro.eaufrance.fr) at variable time steps and were converted into hourly time steps. The studied period extended from September 2000 to September 2013. Since not all stations in the database had all 13 hydrological years of data, 3 years of runoff data was established as a minimum requirement for study (boxplot Figure 5). A total of 389

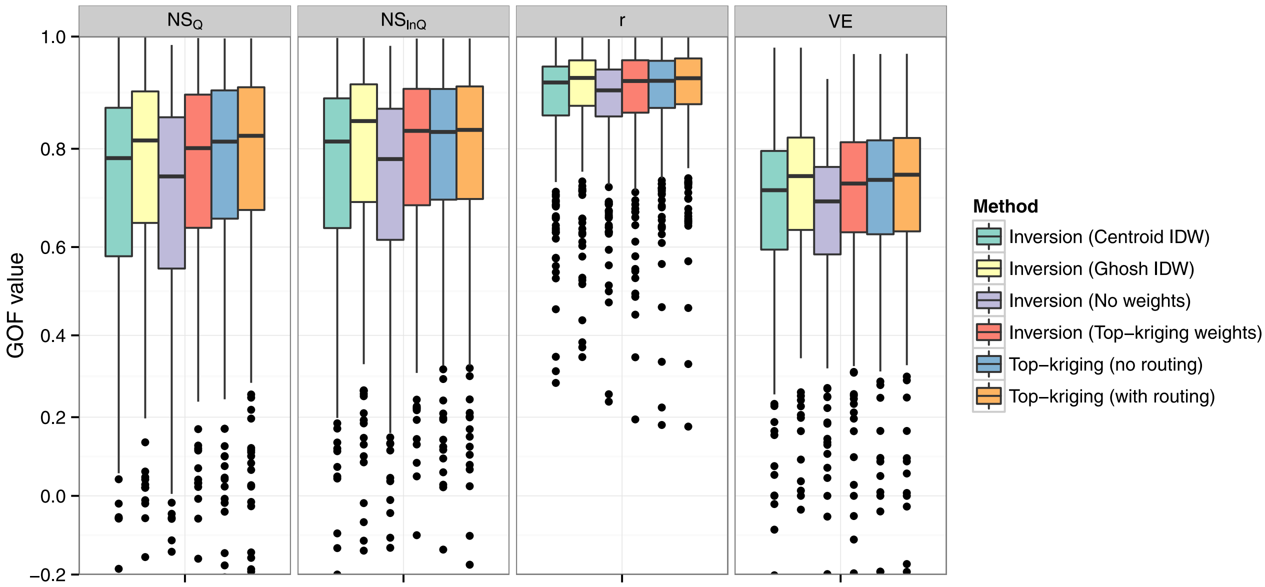

Figure 6. Prediction performance using four criteria. NS_Q: Nash-Suttcliff efficiency, NS_{lnQ}: Nash-Suttcliff efficiency with logarithm transformation, *r*: Pearson correlation, *VE*: volumetric efficiency, IDW: inverse-distance weighting, and GOF: goodness of fit.

catchments were selected for this study. Mean gauge density is 3.6 gauges per 1000 km^2 in the entire study area (4.5, 2.6, and 4.6 gauges per 1000 km^2 in zones 1, 2, and 3, respectively).

4. Results

4.1. Statistical Distribution

Goodness of fit of streamflow predicted for the entire dataset using the geomorphological approach varied by weighting strategy (Figure 6). The worst predictions were obtained when using the simple mathematical mean of the donor catchments (strategy 1). Predictions improved when using IDW based on centroid distances. The best predictions were obtained from the inverse rescaled Ghosh distance weighting.

This demonstrates that introducing more sophisticated weighting strategies improves the skill of the transfer approach. This result differs from *Andréassian et al*. [2012] and *de Lavenne* [2013], who found the simple mathematical mean as the best approach among those tested. This difference in results could be explained by the present study's larger dataset, which yielded a stronger statistical significance. In particular, this improvement is more obvious when dealing with larger catchments (see section 4.3).

Retrieving Top-kriging weights and applying the weights in the geomorphological approach did not improve the goodness of fit, and even produced slightly worse performances. However, the differences were quite small and not significant. Consequently, it does not seem worth the effort to apply the hybrid approach rather than the inverse rescaled Ghosh distance approach. A different choice of variogram, however, could potentially influence this. A scatterplot of the two weighting strategies (Figure 7) indicated that the values of the weights followed a similar trend. However, Top-kriging tended to smooth the weights among donor catchments, whereas the inverse function yielded more contrasting weights (more low and high values). In this way, Top-kriging tends to combine the information of all donor catchments, whereas inverse rescaled Ghosh distance weighting attributes most of the weight to the nearest catchments.

Comparison of goodness-of-fit criteria showed that the weighting strategy seemed to have slightly more influence on high flows (estimated by NS_Q) than low flows (estimated by NS_{lnQ}) and on volume efficiency. Conversely, timing correlation (estimated by *r*) appeared to have similar performance for all inverse-weighting variants. This is because timing correlation depends mostly on velocity, which was the same for all weighting approaches.

Top-kriging was applied with and without routing to consider the time lag in the correlation of two runoff measurements of two different catchments. However, including routing improved performance only slightly,

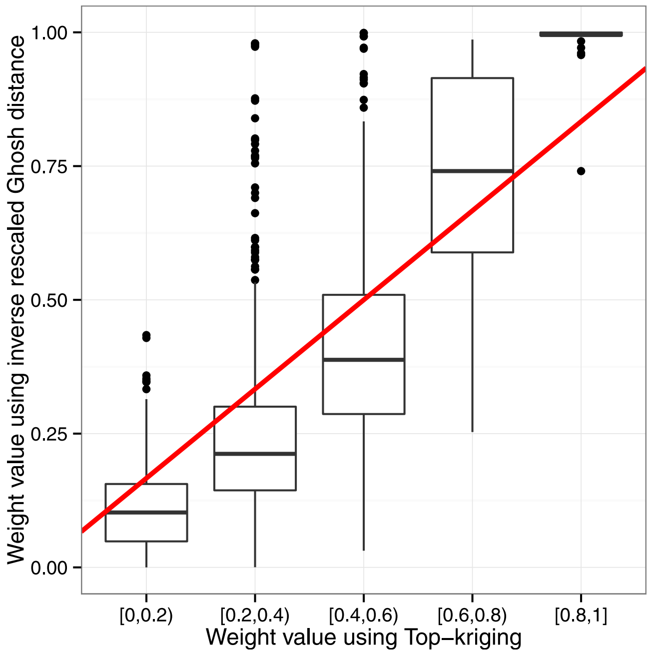

Figure 7. Comparison of optimized weights of Top-kriging to weights calculated using an inverse rescaled Ghosh distance function. Weights are compared for an identical group of donor catchments used for each ungauged catchment.

according to the goodness-of-fit criteria. This result does not differ much from those of *Skøien and Blöschl* [2007], who also observed a small improvement when including a routing routine. The slight improvement may be explained by a poorly estimated time lag. Only one regression was performed for the entire dataset, but time-to-peak may depend on the magnitude of the event and previous conditions. This theory also assumes some degree of homogeneity in the temporal pattern of precipitation (as does the geomorphology-based approach), but this assumption may be invalid, particularly for ungauged headwaters in mountainous catchments. Consequently, not every catchment may benefit from including a routing routine.

Ultimately, the Top-kriging and geomorphology-based approaches provided similar results (Figures 6 and 8). In particular, the geomorphological approach using IDW of the rescaled Ghosh distance performed similarly to Top-kriging with routing for all goodness-of-fit criteria. By having a performance similar to that of Top-kriging, which in other studies often outperformed other regionalization approaches [*Archfield et al.*, 2013; *Viglione et al.*, 2013; *Laaha et al.*, 2014], the geomorphological approach is also likely to outperform these other approaches.

4.2. Spatial Distribution

Spatial analysis of the goodness of fit of predictions demonstrated highly variable performances within region 1 (Figures 9 and 10). This is most likely because the variable hydrology and climate in this mountainous region make predictions more difficult. Rainfall and evapotranspiration have higher spatial gradients in this region than in the other two (Figure 5).

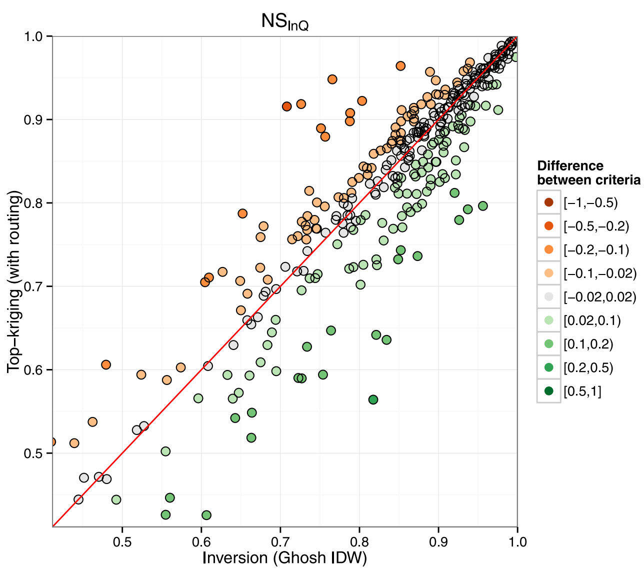

Figure 8. Scatterplot of NS_{lnQ} efficiency criteria between the geomorphological approach (using Ghosh IDW) and Top-kriging (using routing). A map of those differences is provided in supporting information (S1).

A small group of catchments in region 1 (group 1 in Figure 9) is composed of catchments whose performances were lower than those of its neighbors. However, these catchments are largely covered by an urban area (the city of Clermont-Ferrand), which strongly influences discharge. Moreover, these catchments have lower quality data, particularly because of difficulties in delineating them. This illustrates one limitation of both approaches: uncertainties in discharge measurements are also transferred to and influence neighboring catchments.

The influence of dams can also influence prediction performances. For instance, the methods performed particularly poorly in

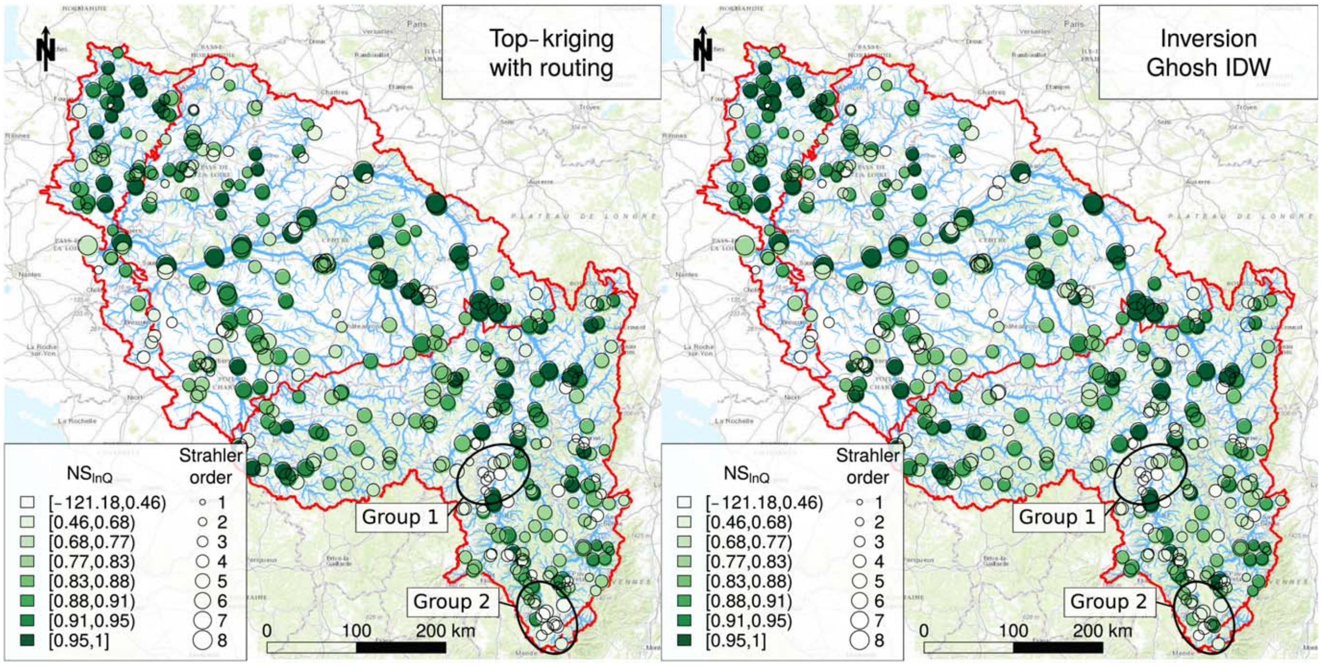

Figure 9. Maps of Nash-Sutcliffe efficiency criteria performed on log-transformed discharges (NS_{lnQ}) for Top-kriging (using routing) and geomorphological modeling (using Ghosh inverse-distance weighting (IDW)).

a series of catchments near Naussac (group 2 in Figure 9). Because of the headwater location of this dam, transfers of the hydrograph are more likely to make predictions based on catchments with contrasting hydrology. Top-kriging, which tends to give larger weights to the nonnearest neighbors than the rescaled Ghosh distance IDW (due to smoother weights, as discussed above (Figure 7)), is thus more influenced by this configuration (lower performances, Figure 9).

In contrast to region 1, region 3 had the best performances (Figure 10), with relatively high NS_Q values homogeneously distributed in space. Region 2 had more spatially variable results. As described in section 3.4, this region of sedimentary rock is influenced locally by aquifers, which can reduce the spatial correlation depending on the size and number of aquifers connected to each catchment's hydrosystem network. Because the region has a lower density of stream gauges, its hydrographs were estimated from more remote donor catchments, which are more likely to differ hydrologically.

Overall, the spatial distribution analysis demonstrates certain limits of approaches that rely only on distances between catchments in geographic space. Even though these distances respect the topology and hydrological organization of catchments, we included no hydrological descriptors other than catchment boundaries to compute them. This can influence performances of regionalization because the hydrographs of some catchments may be estimated by hydrographs of catchments spatially very close but hydrologically very different. Consequently, hydrographs of these catchments cannot interpolate well from the hydrographs of neighboring catchments, particularly those whose hydrological variables vary greatly in space (such as region 1).

This reflects numerous studies on the use of spatial proximity as an indicator of hydrological similarity [*Merz and Blöschl*, 2004; *Blöschl*, 2005; *Merz and Blöschl*, 2005; *Oudin et al.*, 2008, 2010; *Randrianasolo et al.*, 2011]. However, most agree that spatial proximity is most often the best indicator because hydrological similarity assessed through spatial proximity usually reflects the similarity of other characteristics, as expressed by *Sawicz et al.* [2011].

Comparison of the performances of Top-kriging (with routing) and the geomorphological approach (with rescaled Ghosh distance IDW) revealed no spatial pattern in differences between them (Figure 8 and S1 in supporting information). Consequently, neither approach seems more effective for particular regions or types of catchments.

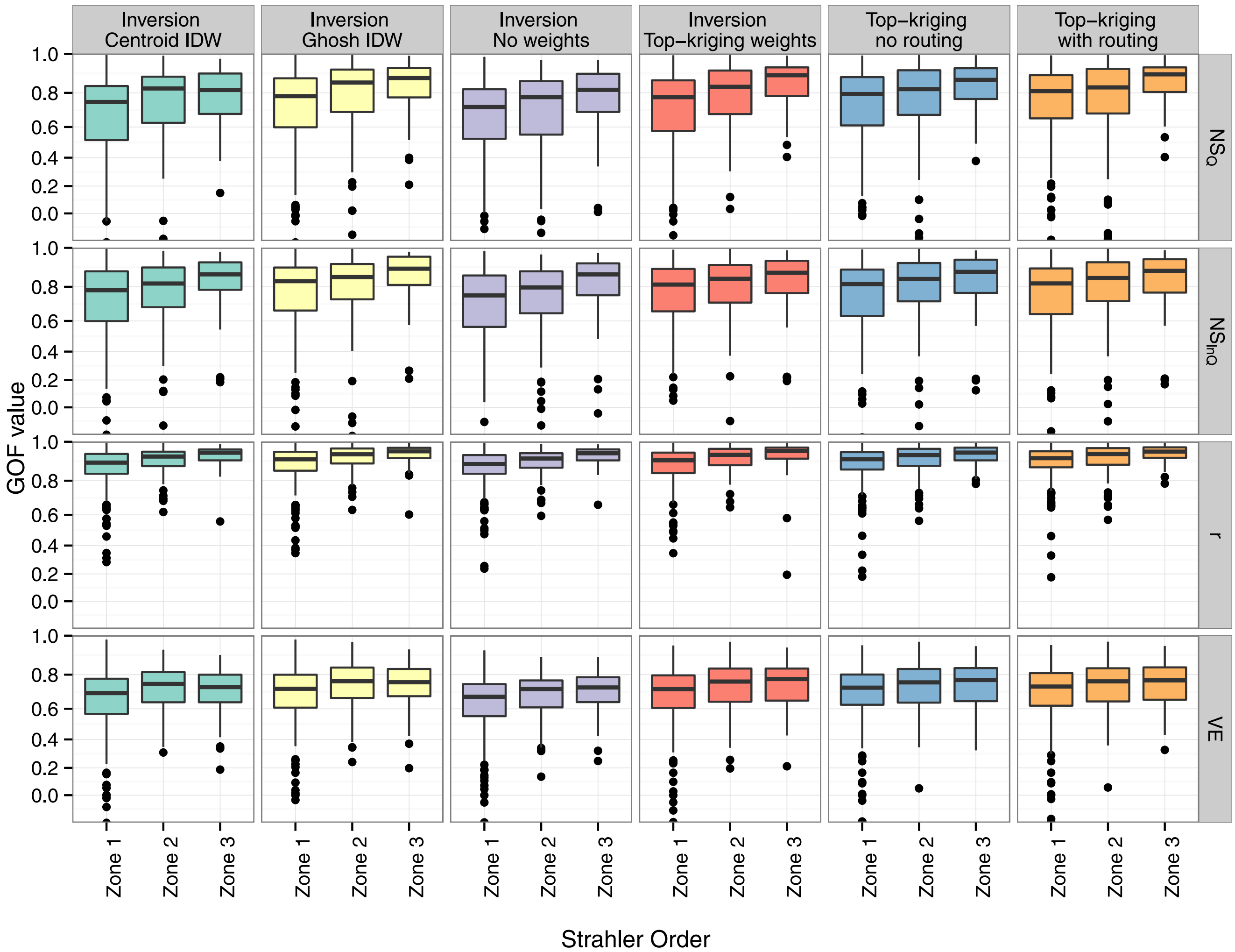

Figure 10. Goodness of fit of predictions by geographic region.

4.3. Performance Drivers

The accuracy of predictions appeared strongly related to catchment size, which is typically related to their relative order in the catchment. Higher Strahler orders had higher performances (Figure 11), which confirms that larger catchments are more predictable than smaller catchments. This is because, first, the hydrograph at the outlet of a large catchment is a smoothed response to a wide diversity of conditions, whereas smaller catchments can exhibit highly specific behavior. Second, large overlaps usually exist between the catchment areas in the ungauged location and the gauges upstream or downstream. This is demonstrated by the mean Ghosh distance as a function of Strahler order (Figure 12), which shows that catchments of higher Strahler order usually have a higher degree of nesting with their donor catchments (lower Ghosh distance). It is interesting to note that the Ghosh distance assesses the gauging density that accounts for the nesting structure (compared to traditional evaluation of the number of stream gauges per unit area, as done by *Parajka et al.* [2015]). From this viewpoint, smaller catchments are less gauged than larger catchments (Figure 12).

The weighting strategy also influenced the accuracy of the transfer of the hydrograph. With equal weights, prediction performances increased from the smallest-order catchments to those of order 5 or 6 (depending on the goodness-of-fit criteria, Figure 11) but then decreased. Also, the centroid-IDW function seemed to reach a threshold in prediction performance, while all other functions improved their efficiency when the size of the ungauged catchment increased. The same threshold of a Strahler order of 5–6 was also observed (Figure 12).

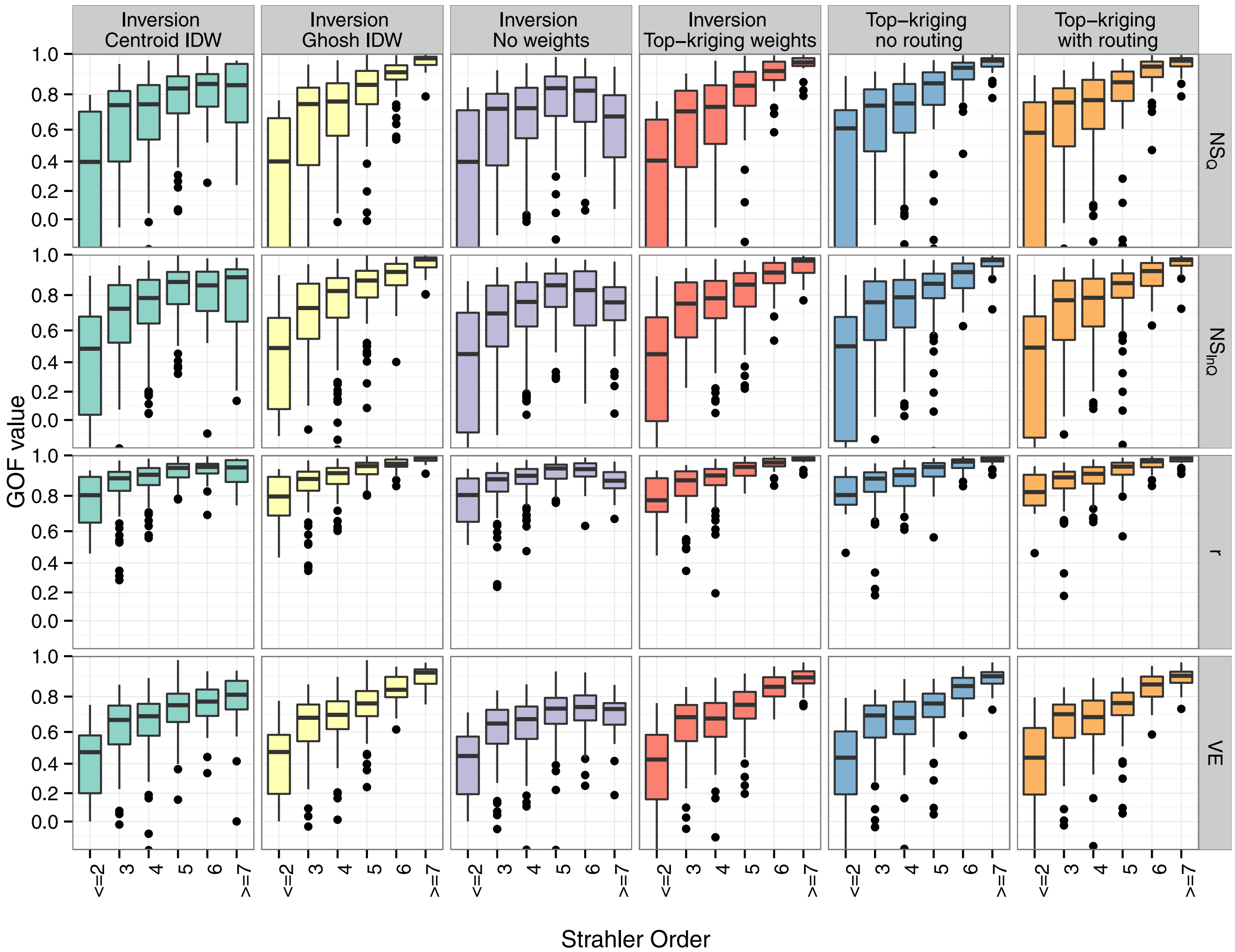

Figure 11. Performance of predictions using four criteria according to catchment Strahler order. NS_Q: Nash-Suttcliff efficiency, NS_{lnQ}: Nash-Suttcliff efficiency with logarithm transformation, *r*: Pearson correlation, *VE*: volumetric efficiency, IDW: inverse-distance weighting, and GOF: goodness of fit.

These results demonstrate that the Ghosh distance, which was used in all other approaches (Ghosh IDW and Top-kriging), is particularly useful for larger catchments. Donor catchments with a high degree of nesting are easier to find for larger catchments (Figure 12). The Ghosh weighting strategies are able to detect these suitable donors, whereas other weighting strategies do not. The equal-weighting approach and the centroid-IDW approach can give unreasonably large weights to catchments that lie close to the centroids but that have a low degree of nesting.

One could conclude that the degree of nesting is the main driver of performance besides the size of the catchment (Figures 11 and 12); however, the relation between prediction efficiency and Ghosh distance to donor catchments (Figure 13) is not straightforward. For a given Strahler order class, the performance does not always decrease when the rescaled Ghosh distance of donor catchments increases. This is only verified for small catchments (Strahler order below 2) and, to a lesser extent, catchments with Strahler orders above 7. For instance, catchments of Strahler order 3 have the worst performances with the closest catchments. This demonstrates that stream-gauging density is an important driver of performance for small headwater catchments, where hydrological variability is high, but is less relevant for larger catchments. Without contradicting the work of *Parajka et al*. [2015], which highlights a clear relationship between Top-kriging performances and stream-gauge density, these results suggest the need to consider the effect of stream-gauge density as a function of catchment size.

Differences between geomorphology-based inversion (Ghosh IDW) and Top-kriging (with routing) approaches did not strongly indicate that one approach could model a certain catchment size better than

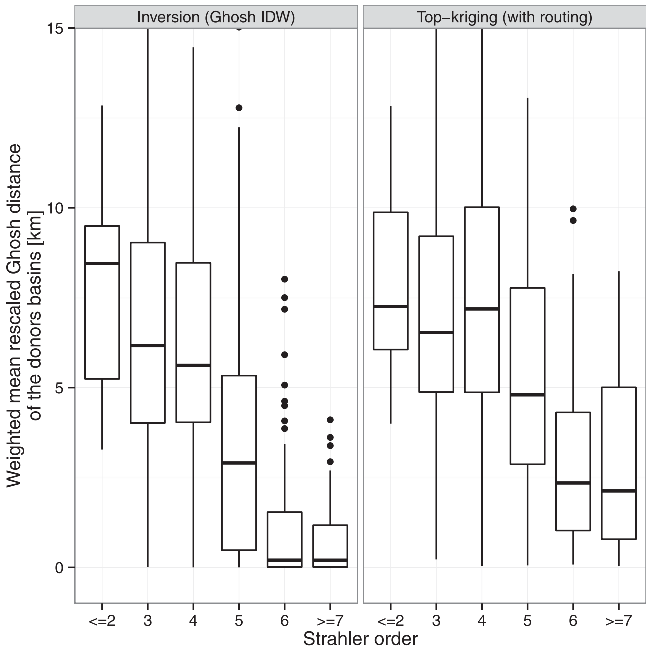

Figure 12. Weighted mean rescaled Ghosh distance between receiver catchments and their five donor catchments. Weights are those used for transferring hydrographs.

the others (Figure 11). Only the NS_Q criteria appeared to demonstrate that the Top-kriging approach provided better results for smaller catchments (Strahler order ≤ 2) than the geomorphological approach. The high variability in hydrological behavior of small catchments seems better addressed by using a variogram instead of a simple IDW approach with the Ghosh distance.

Moreover, the geomorphological approach is better suited to larger catchments. Indeed, hillslope travel time tends to dominate the hydrological response for smaller catchments [*D'Odorico and Rigon*, 2003] even if it is a difficult task to say when it occurs exactly [see for instance, *Lazzaro et al*., 2016; *Rigon et al*., 2016]. For this reason, as donor catchments get smaller, their network transfer function tends to be shorter. The inversion then

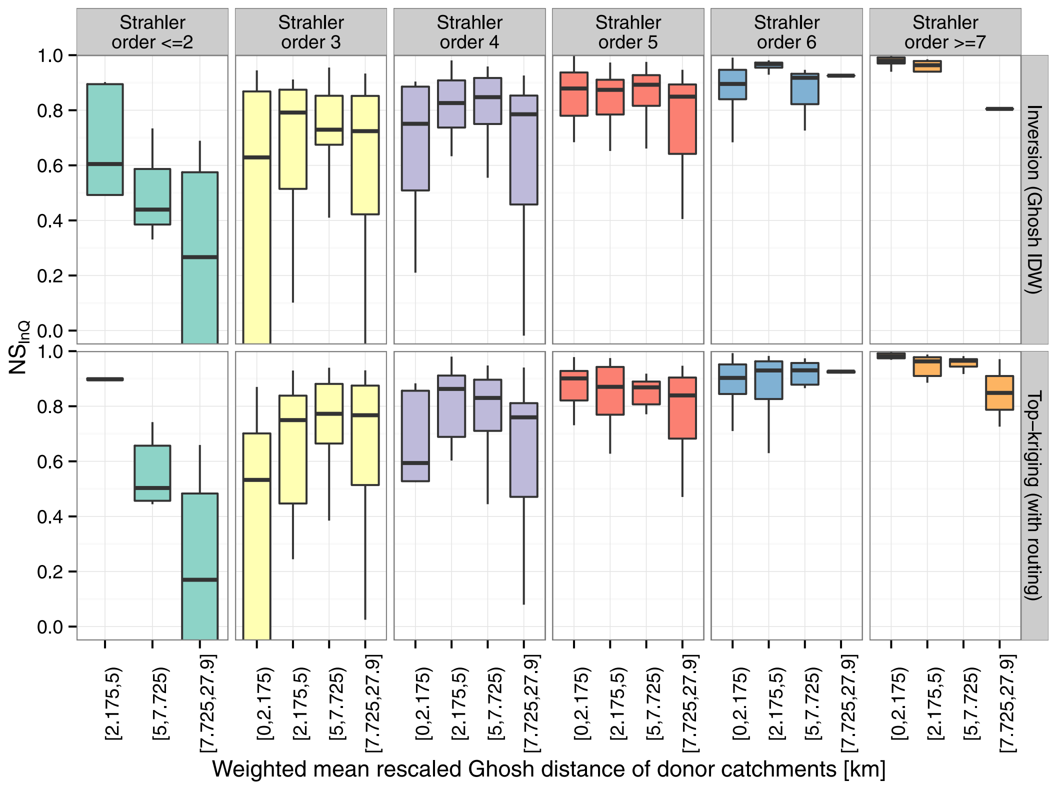

Figure 13. Performance of simulation (using NS_{lnQ} criteria) of receiver catchments according to the weighted mean rescaled Ghosh distance to their five donor catchments. Weights are those used for transferring hydrographs.

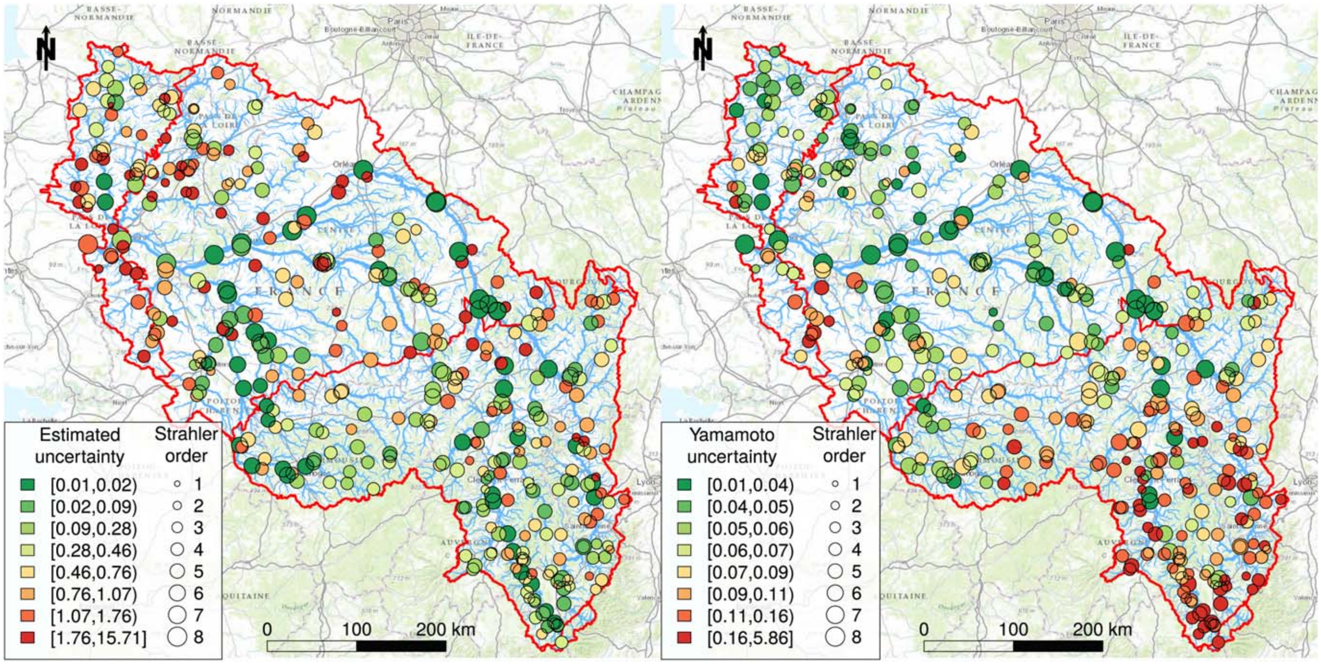

Figure 14. Maps of estimated uncertainty in predictions (coefficient of variation: variance divided by the prediction) using (left) traditional kriging variance and (right) an alternative variance developed by *Yamamoto* [2000].

becomes insignificant because the net rainfall time series tends to be similar to the discharge time series. With insignificant inversion, hydrograph transfer in the two approaches becomes similar, and the main differences in performances can only be explained by weighting strategy, as described in the previous paragraph.

4.4. Prediction Uncertainty

Similar to other kriging methods, Top-kriging has the advantage of estimating the uncertainty in predictions, as a level of confidence in the interpolation. For the time series we predicted in this study, this variance was considered first as an indicator of uncertainty in the entire time series rather than as a prediction of variance for individual time steps, since it was independent of event size. Second, comparison of this kriging variance (Figure 14, left) with the goodness-of-fit indicators of the predictions (Figure 9) showed that their spatial organization is inconsistent. Low and high uncertainties were frequently associated with low and high prediction efficiencies, respectively.

As a consequence, we also examined an alternative variance developed by *Yamamoto* [2000]. Unlike traditional kriging variance, which is based on a general variogram model that is constant for the entire studied region, this variance depends on local variability in the data. It also requires nonnegative weights to assure a positive variance. This variance appeared to better fit the prediction efficiency (Figure 14, right). It was a better indicator in regions with lower prediction efficiency, such as in the upper part of the Loire catchment, where uncertainty was higher.

The geomorphology-based inversion approach analyzes uncertainty from a different perspective. Instead of visualizing the final mean prediction, which combines all gauged catchments' hydrographs, *de Lavenne* [2013] and *de Lavenne and Cudennec* [2015] graphically explored individual transfers (Figure 15). Individual transfers are predictions that result from only one donor catchment. Because each prediction uses the same transfer function for the receiver catchment, differences can come only from net rainfall estimates, which can thus be visualized indirectly (Figure 15). Uncertainty is then estimated from the diverse hydrological responses among the donor catchments. This hydrological heterogeneity (grey envelope in Figure 15) is developed from minimum and maximum values among individual transfers.

This uncertainty does not describe the uncertainty of the model itself but hypothesizes that uncertainty in the prediction increases when donor catchments have different specific discharges. Conversely, reliability

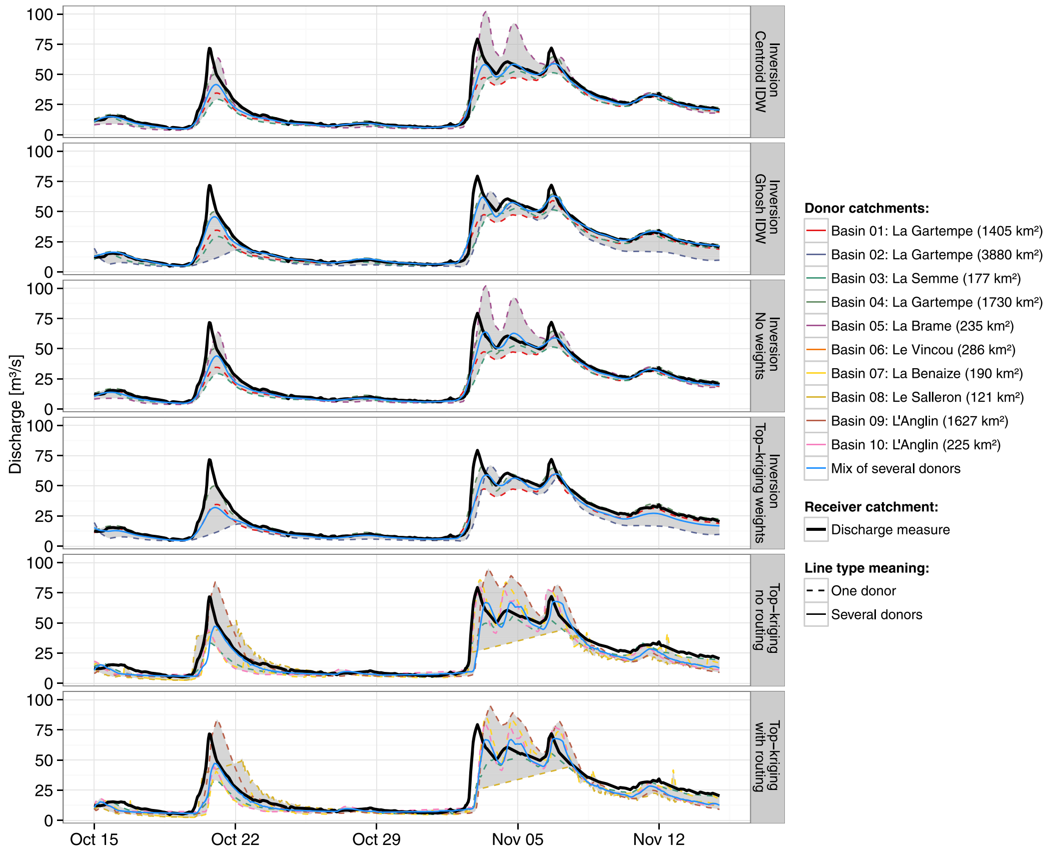

Figure 15. Hydrograph simulation using Top-kriging and inversion, with uncertainty envelopes produced by different donor catchments. Example of the Gartempe River basin (1868 km^2) near Montmorillon, France, from 15 October to 15 November 2012.

of the prediction increases when all gauged catchments have similar specific discharge. This approach reflects the work of *McIntyre et al*. [2005] and *Randrianasolo et al*. [2011], in which ensemble modeling predictions were obtained from neighboring catchments and which are similar to the Yamamoto approach [*Yamamoto*, 2000].

Results demonstrate that the Ghosh distance approach selected the donor catchment better than the centroid-IDW approach (Figure 15). Consequently, the uncertainty envelope narrowed, and the consistency of prediction increased.

Predictions from the geomorphology-based inversion approach appeared smoother than those from Top-kriging (Figure 15). This is because the former estimates an intermediate variable (net rainfall) that is then convoluted with a transfer function that causes this smoothing effect. Top-kriging uses direct discharge observation; thus, the particular shapes of donors' hydrographs are also directly transferred to the ungauged catchment. For this reason, Top-kriging sometimes has a wider prediction envelope. However, a similar smoothing effect would potentially occur if full spatiotemporal kriging (instead of only spatial kriging) was implemented in Top-kriging.

The predicted hydrographs also demonstrate that the timing of flood events was not described identically by each neighbor when using Top-kriging. It is possible to transfer different flood-peak timings even though the routing attempts to recenter the hydrograph according to estimates of catchment lag times. Calculating the weighted mean discharge may be problematic if different timings are combined. Multiple flood peaks may result from averaging time series that have different timing. Conversely, inversion predicts higher agreement in timing because each ungauged catchment has its own unique network transfer function that is used for each transferred hydrograph. However, for both approaches, estimating flood timing requires assuming spatially homogeneous rainfall.

10.1002/2016WR018716

5. Discussion

5.1. Founding Principles

Despite having similar performances, Top-kriging and geomorphology-based inversion approaches differ in their founding principles. Top-kriging adapts traditional kriging to hydrological support. It takes advantage of geostatistics that produce the best linear unbiased estimators (BLUE) [*Journel and Huijbregts*, 1978]. However, these approaches assume stationarity, which is not fully respected over the spatiotemporal domain. Consequently, it may be necessary to create multiple variograms for each homogeneous region. Top-kriging thus mainly focuses on constructing a variogram model.

Conversely, the geomorphology-based inversion approach uses a model that is not based on a statistical description of discharge but on a geomorphological description of each catchment. It uses a well-known family of transfer functions and takes advantage of easily observable catchment features to provide a robust modeling approach. It is also based on inverse-modeling techniques to estimate and use net rainfall as an intermediate variable, while Top-kriging predicts directly from discharge measurements. Net rainfall cannot be compared to any measurements, which questions the physical meaning of the time series. Among other issues, solutions of inverse models may be subject to oscillations.

Despite differences in how the methods were developed, they share certain properties that can explain their similar behaviors. Top-kriging point variograms examine properties of unobserved runoff generation at the point scale. This runoff generation can be seen as a different way to describe the net rainfall of the geomorphology-based model. The approaches differ in that Top-kriging spatially convolutes statistical properties of net rainfall to find weights of runoff observations, whereas the geomorphology-based approach interpolates net rainfall directly and spatiotemporally convolutes it using the UH. We would expect the geomorphology-based inversion approach, by using UH, to better predict the shape of hydrographs, but this was not detectable in the performance indicators.

5.2. Ease of Application

One advantage of the geomorphology-based approach is that it can be applied using only a single neighbor (as originally designed) while still preserving certain characteristics of the ungauged catchment by convoluting net rainfall with the UH. This can address many situations for points of interest, such as when only one station is within a practical range. Like any other geostatistical approach, Top-kriging needs an adequate number of catchments to estimate the variogram, but can, like all distance-based methods, also make a prediction based on a single neighbor. However, this prediction would reproduce exactly the same specific discharge, possibly with a phase shift due to the routing routine, but without the shape shift that comes from using multiple UHs.

5.3. Flexibility and Perspectives for Evolution

In terms of flexibility, Top-kriging has a nonnegligible advantage over the geomorphological approach. Top-kriging can easily be used to estimate flow statistics (and is more widely used for this purpose), whereas the geomorphological approach is mainly designed for interpolating time series. So far, the only way to estimate flow statistics using the geomorphological approach is to derive them from the predicted discharge. Further investigation is needed to know whether this approach would provide satisfactory results.

An intermediate variable, i.e., net rainfall, is the geomorphology-based approach's solution to solve the scaling issue inherent in transfer of hydrographs between catchments of different sizes. This net rainfall can then be transferred to neighboring catchments independent of scale. Top-kriging uses specific discharge and regularizes the variogram to address the scaling issue.

Despite difficulties inherent in inverse modeling, estimating net rainfall from discharge measurements also opens new perspectives, such as corrections according to spatiotemporal rainfall variability [*de Lavenne*, 2013]. This aspect can also be considered in Top-kriging, but only by using a spatiotemporal trend model [*Montanari*, 2005]. In contrast, net rainfall estimated from a geomorphology-based approach can be compared to rainfall measurements more directly.

It is also important to note that Top-kriging differs from the geomorphological approach by treating the dataset as a whole, by applying a global variogram model, whereas the geomorphological approach models each catchment more separately (even though it also uses a single method to estimate weights). Each catchment has its own transfer function that controls the shape of each simulated hydrograph. Conversely, Top-kriging predicts the shape of one hydrograph from the shapes of neighboring hydrographs, even though the routing in Top-kriging is adapted to individual catchments. Top-kriging focuses more on measurements, while the geomorphological approach requires more assumptions about modeling water transfer at the catchment scale. It would be easy for it to use more advanced transfer functions, depending upon available knowledge and data. For instance, it can consider dispersion [*Rinaldo et al*., 1991] explicitly, whereas the Top-kriging approach considers this aspect more implicitly [*Skøien et al*., 2006; *Skøien and Blöschl*, 2007].

With only a few improvements to include routing, the results also highlight that both approaches could better consider variability in flow velocity; however, other factors may be more important or easier to use. For instance, differences in runoff production are an important issue that has not yet been examined. Doing so would require estimating hillslope behavior, which would mean using a much more complex hydrosystem model.

5.4. Common Traits

Finally, the results demonstrate that both approaches achieve similar performances when using the same description of distance between catchments, i.e., the Ghosh distance. However, the weights from Top-kriging did not improve performance when applied to the geomorphological model. Combining the simple IDW approach with Ghosh distances provides performance similar to that of Top-kriging with a calibrated variogram. This emphasizes that measuring distances between catchments (physically and hydrologically) is one of the most important aspects on which to focus.

The weakness of both approaches is apparent for small catchments, which have higher variability in hydrological behavior than larger catchments. Any approach that attempts to identify a similar catchment using only geographic distance has strong limitations. This can be partly solved with better understanding of hydrological drivers; however, it is also likely that assumptions of homogeneous net rainfall in the geomorphological approach and the generated runoff in the Top-kriging approach are less applicable for smaller catchments. For other methods, regionalization based on regression has the advantage of describing more explicitly catchment characteristics that are related to a specific expected hydrological response.

6. Conclusion

Among regionalization studies, only a few approaches transfer weighted time series observations to ungauged locations. Driven by the idea of maximizing data assimilation with a minimum of model development, we compared two of these observation-based approaches for a large dataset of 389 catchments spread over the Loire River basin, the largest French basin (110,000 km^2 at the outlet of Mont-Jean-sur-Loire).

The first is the Top-kriging approach based on the work of *Skøien et al*. [2006] and *Skøien and Blöschl* [2007], which was applied in a slightly modified form using the rtop package. This method is often compared to other regionalization techniques, such as regression [*Archfield et al*., 2013; *Laaha et al*., 2014], for estimating statistical catchment characteristics, and the regionalized hydrological model, for predicting continuous streamflow [*Viglione et al*., 2013; *Parajka et al*., 2015]. In these studies, Top-kriging outperformed other regionalization approaches.

The second approach implemented, initiated by *Cudennec* [2000] in small semiarid Tunisian basins and recently applied in France by *de Lavenne et al*. [2015], relies on inverting a robust geomorphology-based transfer function of runoff through the river network. This study demonstrates that both approaches can be applied in a similar manner. They are similar in their need for calibration (with estimated streamflow velocity) and in how distances (as a proxy of hydrological similarity) are calculated between one gauged and one ungauged catchment.

Despite these common traits, each approach emerges from a different school of thought. Top-kriging is based on geostatistics and uses statistical correlation to optimize weights. In contrast, the second approach comes from geomorphology-based hydrological modeling, widely used to make predictions about ungauged catchments. It uses easily observable catchment characteristics to describe the hydrograph of each catchment separately. The ability to treat each catchment more individually than in Top-kriging makes it possible, in theory, to include different levels of knowledge for each catchment. It does not benefit, however, from the strength of statistical optimization for choosing and weighting the donor catchment, which is the key challenge in both approaches. The final results from predictions over 13 hydrological years demonstrate similar performances of both approaches, showing that the geomorphology-based inversion approach is as reliable as the well-known Top-kriging approach. This was achieved despite the slightly simpler weighting function of the geomorphological approach based on Ghosh inverse-distance weighting.

This study emphasizes the advantage of the Ghosh distance [*Ghosh*, 1951; *Gottschalk*, 1993; *Gottschalk et al*., 2011] for choosing and weighting gauged catchments as donors of observed streamflow to ungauged locations. The advantage of this weighting strategy differs from that in the study by *Andréassian et al*. [2012], in which the simple mathematical mean of the neighboring catchments performed better. This weighting strategy appears particularly relevant for catchments with Strahler orders above five, i.e., in which nested catchment structures are more significant.

Acknowledgments
This research was funded by Etablissement Public Loire, Agence de l'eau Loire Bretagne, European Regional Development Fund, and the "Eutrophisation-Trend "project. The discharge data used for this study are freely provided by the French Banque hydro database (www.hydro.eaufrance.fr).

References

Andréassian, V., J. Lerat, N. Le Moine, and C. Perrin (2012), Neighbors: Nature's own hydrological models, *J. Hydrol.*, *414*, 49–58, doi:10.1016/j.jhydrol.2011.10.007.
Aouissi, J., J. C. Pouget, H. Boudhraâ, G. Storer, and C. Cudennec (2013), Joint spatial, topological and scaling analysis framework of river-network geomorphometry, *Géomorphol. Relief Processus Environ.*, *1*, 7–16, doi:10.4000/geomorphologie.10082.
Archfield, S. A., A. Pugliese, A. Castellarin, J. O. Skøien, and J. E. Kiang (2013), Topological and canonical kriging for design flood prediction in ungauged catchments: An improvement over a traditional regional regression approach?, *Hydrol. Earth Syst. Sci.*, *17*, 1575–1588, doi:10.5194/hess-17-1575-2013.
Beven, K., and E. F. Wood (1993), Flow routing and the hydrological response of channel networks, in *Channel Network Hydrology*, pp. 99–128, John Wiley, Chichester, U. K.
Blöschl, G. (2005), Rainfall-runoff modeling of ungauged catchments, in *Encyclopedia of Hydrological Sciences*, pp. 2061–2079, John Wiley, Hoboken, N. J., doi:10.1002/0470848944.hsa140.
Blöschl, G., and M. Sivapalan (1995), Scale issues in hydrological modelling: A review, *Hydrol. Processes*, *9*, 251–290, doi:10.1002/hyp.3360090305.
Blöschl, G., M. Sivapalan, T. Wagener, A. Viglione, and H. H. G. Savenije (2013), *Runoff Prediction in Ungauged Basins. Synthesis Across Processes, Places and Scales*, Cambridge Univ. Press, Cambridge, U. K.
Boudhraâ, H. (2007), Modélisation pluie-débit à base géomorphologique en milieu semi-aride rural tunisien: association d'approches directes et inverses, PhD thesis, Inst. Natl. Agron. de Tunisie à Tunis, Tunis, Tunisia.
Boudhraâ, H., C. Cudennec, M. Slimani, and H. Andrieu (2006), Inversion d'une modélisation de type hydrogramme unitaire à base géomorphologique: interprétation physique et première mise en oeuvre, *IAHS Publ.*, 303, 391－399.
Boudhraâ, H., C. Cudennec, M. Slimani, and H. Andrieu (2009), Hydrograph transposition between basins through a geomorphology-based deconvolution-reconvolution approach, *IAHS Publ.*, *333*, 76–83.
Cressie, N. (1993), *Statistics for Spatial Data: Wiley Series in Probability and Statistics*, Wiley-Interscience, N. Y.
Criss, R. E., and W. E. Winston (2008), Do Nash values have value? Discussion and alternate proposals, *Hydrol. Processes*, *22*, 2723–2725, doi:10.1002/hyp.7072.
Cudennec, C. (2000), Description mathématique de l'organisation du réseau hydrographique et modélisation hydrologique, PhD thesis, Ecole Natl. Supérieure Agron. de Rennes, Rennes, France.
Cudennec, C. (2007), On width function-based unit hydrographs deduced from separately random self-similar river networks and rainfall variability: Discussion of ''Coding random self-similar river networks and calculating geometric distances: 1. General methodology'' and ''2. Application to runoff simulations,'' *Hydrol. Sci. J.*, *52*, 230–237, doi:10.1623/hysj.52.1.230.
Cudennec, C., and Y. Fouad (2006), Structural patterns in river network organization at both infra- and supra-basin levels: The case of a granitic relief, *Earth Surf. Processes Landforms*, *31*, 369–381, doi:10.1002/esp.1275.
Cudennec, C., Y. Fouad, I. S. Gatot, and J. Duchesne (2004), A geomorphological explanation of the unit hydrograph concept, *Hydrol. Processes*, *18*, 603–621, doi:10.1002/hyp.1368.
de Lavenne, A. (2013), Modélisation hydrologique à base géomorphologique de bassins versants non jaugés par régionalisation et transposition d'hydrogramme, PhD thesis, Agrocampus-Ouest Rennes, Rennes, France.
de Lavenne, A., and C. Cudennec (2015), Prediction of streamflow from the set of basins flowing into a coastal bay, *Proc. Int. Assoc. Hydrol. Sci.*, *365*, 55–60, doi:10.5194/piahs-365-55-2015.
de Lavenne, A., C. Cudennec, and H. Boudhraâ (2015), Streamflow prediction in ungauged basins through geomorphology-based hydrograph transposition, *Hydrol. Res.*, *46*(2), 291–302, doi:10.2166/nh.2013.099.
D'Odorico, P., and R. Rigon (2003), Hillslope and channel contributions to the hydrologic response, *Water Resour. Res.*, *39*(5), 1113, doi:10.1029/2002WR001708.
Farmer, W. H. (2016), Ordinary kriging as a tool to estimate historical daily streamflow records, *Hydrol. Earth Syst. Sci. Discuss.*, *2016*, 1–23, doi:10.5194/hess-2015-536.
Ghosh, B. (1951), Random distances within a rectangle and between two rectangles, *Bull. Calcutta Math. Soc.*, *43*, 17–24.
Giannoni, F., G. Roth, and R. Rudari (2003a), Can the behaviour of different basins be described by the same model's parameter set? A geomorphologic framework, *Phys. Chem. Earth*, *28*, 289–295, doi:10.1016/S1474-7065(03)00040-8.
Giannoni, F., J. A. Smith, Y. Zhang, and G. Roth (2003b), Hydrologic modeling of extreme floods using radar rainfall estimates, *Adv. Water. Resour.*, *26*, 195–203, doi:10.1016/S0309-1708(02) 00091-X.
Gottschalk, L. (1993), Interpolation of runoff applying objective methods, *Stochastic Hydrol. Hydraul.*, *7*, 269–281, doi:10.1007/BF01581615.
Gottschalk, L., E. Leblois, and J. O. Skøien (2011), Distance measures for hydrological data having a support, *J. Hydrol.*, *402*, 415–421, doi:10.1016/j.jhydrol.2011.03.020.
He, Y., A. Bárdossy, and E. Zehe (2011), A review of regionalisation for continuous streamflow simulation, *Hydrol. Earth Syst. Sci.*, *15*, 3539–3553, doi:10.5194/hess-15-3539-2011.

Hrachowitz, M., et al. (2013), A decade of Predictions in Ungauged Basins (PUB)—A review, *Hydrol. Sci. J.*, *58*, 1198–1255, doi:10.1080/02626667.2013.803183.

Isaak, D. J., et al. (2014), Applications of spatial statistical network models to stream data, *WIREs Water*, *1*, 277–294, doi:10.1002/wat2.1023.

Jasiewicz, J., and M. Metz (2011), A new GRASS GIS toolkit for Hortonian analysis of drainage networks, *Comput. Geosci.*, *37*, 1162–1173, doi:10.1016/j.cageo.2011.03.003.

Journel, A. G., and C. J. Huijbregts (1978), *Mining Geostatistics*, Academic Press, London, U. K.

Kyriakidis, P. C., and A. G. Journel (1999), Geostatistical space–time models: A review, *Math. Geol.*, *31*, 651–684, doi:10.1023/A:1007528426688.

Laaha, G., J. Skøien, and G. Blöschl (2014), Spatial prediction on river networks: Comparison of Top-kriging with regional regression, *Hydrol. Processes*, *28*, 315–324, doi:10.1002/hyp.9578.

Lazzaro, M. D., A. Zarlenga, and E. Volpi (2016), Understanding the relative role of dispersion mechanisms across basin scales, *Adv. Water Resour.*, *91*, 23–36, doi:10.1016/j.advwatres.2016.03.003.

McIntyre, N., H. Lee, H. Wheater, A. Young, and T. Wagener (2005), Ensemble predictions of runoff in ungauged catchments, *Water Resour. Res.*, *41*, W12434, doi:10.1029/2005WR004289.

Menke, W. (1989), *Geophysical Data Analysis: Discrete Inverse Theory*, vol. 45, Academic Press, San Diego, Calif.

Merz, R., and G. Blöschl (2004), Regionalisation of catchment model parameters, *J. Hydrol.*, *287*, 95–123, doi:10.1016/j.jhydrol.2003.09.028.

Merz, R., and G. Blöschl (2005), Flood frequency regionalisation—Spatial proximity vs. catchment attributes, *J. Hydrol.*, *302*, 283–306, doi:10.1016/j.jhydrol.2004.07.018.

Montanari, A. (2005), Deseasonalisation of hydrological time series through the normal quantile transform, *J. Hydrol.*, *313*, 274–282, doi:10.1016/j.jhydrol.2005.03.008.

Müller, M. F., and S. E. Thompson (2015), TopREML: A topological restricted maximum likelihood approach to regionalize trended runoff signatures in stream networks, *Hydrol. Earth Syst. Sci.*, *19*, 2925–2942, doi:10.5194/hess-19-2925-2015.

Naden, P. S. (1992), Spatial variability in flood estimation for large catchments: The exploitation of channel network structure, *Hydrol. Sci. J.*, *37*, 53–71, doi:10.1080/02626669209492561.

Nagel, D., J. M. Buffington, and C. Luce (2011), A simple drainage enforcement procedure for estimating catchment area using DEM data, paper presented at NW GIS User Conference, Boise, Idaho, 17–21 Oct. [Available at http://boise2011.nwgis.org/sessions/simple-drainage-enforcement-procedure-estimating-catchment-area-using-dem-data.html.]

Nash, J. E. and J. V. Sutcliffe (1970), River flow forecasting through conceptual models part I — A discussion of principles, *J. Hydrol.*, *10*(3), 282–290.

Oudin, L., V. Andréassian, C. Perrin, C. Michel, and N. Le Moine (2008), Spatial proximity, physical similarity, regression and ungaged catchments: A comparison of regionalization approaches based on 913 French catchments, *Water Resour. Res.*, *44*, W03413, doi:10.1029/2007WR006240.

Oudin, L., A. Kay, V. Andréassian, and C. Perrin (2010), Are seemingly physically similar catchments truly hydrologically similar?, *Water Resour. Res.*, *46*, W11558, doi:10.1029/2009WR008887.

Parajka, J., R. Merz, J. O. Skøien, and A. Viglione (2015), The role of station density for predicting daily runoff by Top-kriging interpolation in Austria, *J. Hydrol. Hydromech.*, *63*, 228–234, doi:10.1515/johh-2015-0024.

Patil, S., and M. Stieglitz (2012), Controls on hydrologic similarity: Role of nearby gauged catchments for prediction at an ungauged catchment, *Hydrol. Earth Syst. Sci.*, *16*, 551–562, doi:10.5194/hess-16-551-2012.

R Core Team (2015), *R: A Language and Environment for Statistical Computing*, R Found. for Stat. Comput., Vienna.

Randrianasolo, A., M. H. Ramos, and V. Andréassian (2011), Hydrological ensemble forecasting at ungauged basins: Using neighbour catchments for model setup and updating, *Adv. Geosci.*, *29*, 1–11, doi:10.5194/adgeo-29-1-2011.

Rigon, R., M. Bancheri, G. Formetta, and A. de Lavenne (2016), The geomorphological unit hydrograph from a historical-critical perspective, *Earth Surf. Processes Landforms*, *41*, 27–37, doi:10.1002/esp.3855.

Rinaldo, A., A. Marani, and R. Rigon (1991), Geomorphological dispersion, *Water Resour. Res.*, *27*, 513–525, doi:10.1029/90WR02501.

Robinson, J. S., M. Sivapalan, and J. D. Snell (1995), On the relative roles of hillslope processes, channel routing, and network geomorphology in the hydrologic response of natural catchments, *Water Resour. Res.*, *31*, 3089–3101, doi:10.1029/95WR01948.

Rodriguez, F., C. Cudennec, and H. Andrieu (2005), Application of morphological approaches to determine unit hydrographs of urban catchments, *Hydrol. Processes*, *19*, 1021–1035, doi:10.1002/hyp.5643.

Sauquet, E., L. Gottschalk, and I. Krasovskaia (2008), Estimating mean monthly runoff at ungauged locations: An application to France, *Hydrol. Res.*, *39*, 403–423, doi:10.2166/nh.2008.331.

Sawicz, K., T. Wagener, M. Sivapalan, P. A. Troch, and G. Carrillo (2011), Catchment classification: Empirical analysis of hydrologic similarity based on catchment function in the eastern USA, *Hydrol. Earth Syst. Sci.*, *15*, 2895–2911, doi:10.5194/hess-15-2895-2011.

Sivapalan, M., et al. (2003), IAHS Decade on Predictions in Ungauged Basins (PUB), 2003–2012: Shaping an exciting future for the hydrological sciences, *Hydrol. Sci. J.*, *48*, 857–880, doi:10.1623/hysj.48.6.857.51421.

Skøien, J. O., and G. Blöschl (2006), Catchments as space-time filters—A joint spatio-temporal geostatistical analysis of runoff and precipitation, *Hydrol. Earth Syst. Sci.*, *10*, 645–662, doi:10.5194/hess-10-645-2006.

Skøien, J. O., and G. Blöschl (2007), Spatiotemporal topological kriging of runoff time series, *Water Resour. Res.*, *43*, W09419, doi:10.1029/2006WR005760.

Skøien, J. O., R. Merz, and G. Blöschl (2006), Top-kriging—Geostatistics on stream networks, *Hydrol. Earth Syst. Sci.*, *10*, 277–287, doi:10.5194/hess-10-277-2006.

Skøien, J. O., G. Blöschl, G. Laaha, E. Pebesma, J. Parajka, and A. Viglione (2014), rtop: An R package for interpolation of data with a variable spatial support, with an example from river networks, *Comput. Geosci.*, *67*, 180–190, doi:10.1016/j.cageo.2014.02.009.

Tarantola, A., and B. Valette (1982), Inverse problems: Quest for information, *J. Geophys.*, *50*, 150–170.

Vandewiele, G., C.-Y. Xu, and W. Huybrechts (1991), Regionalisation of physically-based water balance models in Belgium. Application to ungauged catchments, *Water Resour. Manage.*, *5*, 199–208, doi:10.1007/BF00421989.

Viglione, A., J. Parajka, M. Rogger, J. L. Salinas, G. Laaha, M. Sivapalan, and G. Blöschl (2013), Comparative assessment of Predictions in Ungauged Basins—Part 3: Runoff signatures in Austria, *Hydrol. Earth Syst. Sci.*, *17*, 2263–2279, doi:10.5194/hess-17-2263-2013.

Yamamoto, J. (2000), An alternative measure of the reliability of ordinary kriging estimates, *Math. Geol.*, *32*, 489–509, doi:10.1023/A:1007577916868.

Yang, D., S. Herath, and K. Musiake (2002), A hillslope-based hydrological model using catchment area and width functions, *Hydrol. Sci. J.*, *47*, 49–65, doi:10.1080/02626660209492907.